

# Development of a Process Simulation Model for Energy Analysis of Hydrogen Production from Underground Coal Gasification (UCG)

**Aman Verma, Babatunde Olateju, Amit Kumar<sup>1</sup>, Rajender Gupta**

4-9 Mechanical Engineering Building, Department of Mechanical Engineering,  
University of Alberta, Edmonton, Alberta, Canada, T6G2G8

## Highlights

- Development of energy balance model for H<sub>2</sub> production from UCG with CCS
- Estimation of coal-to-H<sub>2</sub> conversion efficiency in UCG-syngas based plant
- Sensitivity of key UCG parameters characterized

---

<sup>1</sup> Corresponding author. Tel.: +1-780-492-7797; fax: +1-780-492-2200.

E-mail address: [Amit.Kumar@ualberta.ca](mailto:Amit.Kumar@ualberta.ca) (A. Kumar).



## **Abstract**

This paper presents a model to perform energy balances and estimate hydrogen conversion efficiency from UCG-based syngas. The model was developed for H<sub>2</sub> production from UCG-based syngas with and without CCS, along with the co-production of electricity and steam in a conventional combined cycle plant. In this paper, at base case conditions (H<sub>2</sub>O-to-O<sub>2</sub> injection ratio of 2 and a steam-to-carbon ratio of 3), the coal-to-H<sub>2</sub> conversion efficiency is estimated to be 58.1% for UCG with and without CCS. For the plant configuration involving no CCS, in addition to H<sub>2</sub> production, approximately 4.7% of coal energy is converted to electricity that is exported to the grid. In the case of UCG-CCS, a minor energy penalty is incurred; wherein the electrical energy exported per unit coal energy is around 2.4%, with a CO<sub>2</sub> capture efficiency of 91.6% being achieved. The H<sub>2</sub> conversion efficiency decreases with rise in H<sub>2</sub>O-to-O<sub>2</sub> injection ratio, but increases with fall in steam-to-carbon ratio. Effect of ground water influx in UCG on the H<sub>2</sub> conversion efficiency is minor, whereas H<sub>2</sub> separation efficiency in the pressure swing adsorption (PSA) unit has a major effect.

## **Keywords**

Underground coal gasification (UCG); modeling; energy analysis; hydrogen production; Carbon capture and sequestration (CCS)

## Nomenclature

## 1. Introduction

Canadian crude oil production from the oil sands is projected to rise from 1.8 million barrels per day (bpd) in 2012 to 3.2 and 5.2 million bpd in 2020 and 2030, respectively [1]. The production of hydrogen (H<sub>2</sub>), required to upgrade bitumen to synthetic crude oil (SCO), will increase in a similar fashion. Around 2.52 GJ of H<sub>2</sub> energy is required to upgrade one cubic meter of bitumen to SCO [2]. Steam methane reforming (SMR) is the dominant H<sub>2</sub> production pathway in Alberta and leads to a significant amount of greenhouse house (GHG) emissions, from 8.9-14.21 kg of CO<sub>2</sub>e per kg of H<sub>2</sub> produced [2-8]. To put things into perspective, H<sub>2</sub> production from SMR accounts for around 43% of the total well-to-upgrading<sup>2</sup> GHG emissions in the Canadian oils sands industry [2]. In 2010, the Alberta oils sands industry contributed around 23% to Alberta's total GHG emissions [9]. With a focus on reduction of GHG emissions, the Government of Alberta has set a target of a 50% reduction in projected business-as-usual GHG emissions in 2050, which is around 200 million tonnes in GHG emissions reduction [9]. Therefore, there is justification to explore and study an alternate, less GHG-intensive, hydrogen production pathway for the bitumen upgrading industry.

Coal reserves in Alberta are estimated to be in the range of 2 to 3 trillion tons (Tt) [10-13]. Of the total reserves, there is the potential to recover around 0.62 Tt (or 25% of total reserves) by surface and underground mining [13]. There is an opportunity to retrieve the

---

<sup>2</sup> Well-to-upgrading emissions are those associated with bitumen extraction and upgrading to SCO. In absolute numbers, 0.25 tonnes of CO<sub>2</sub> will be emitted if SMR is used to produce the required amount of H<sub>2</sub> to upgrade one cubic meter of bitumen [2-6].

remaining 75% of the un-minable coal reserves<sup>3</sup> through technology like underground coal gasification (UCG) [12, 14]. In UCG, gasifying agents ( a combination of either water and oxygen, steam and air, steam and oxygen, or water and air) are injected into a coal seam, and syngas is produced through chemical reactions that normally occur in surface coal gasifiers [15, 16]. This produced syngas can be used to produce electricity, hydrogen, liquid fuels, etc. [15, 16]. In a world of anthropogenic induced climate change, UCG has been deliberated as a clean coal conversion technology and a carbon neutral energy pathway [7]. This is due to the fact that while in operation, UCG does not compromise the economic viability and maintains a negligible GHG footprint, especially when combined with CCS [7, 17]. UCG is not only a pragmatic technology for clean coal conversion but also has several economic advantages over surface coal gasification (SCG) [14, 15, 18, 19]. UCG significantly reduces the cost of upstream operations such as coal mining, coal handling, coal transport, and coal gasifiers, and leads to low fugitive emissions, low dust, no ash residues, and reduced noise pollution [14, 15, 18, 19]. However, implementation of UCG-CCS technology on an industrial scale remains a challenge in order to gain the merits over other fossil fuel based pathways, especially SMR, for H<sub>2</sub> production. Some of the challenges to adopt UCG technology as an energy production pathway comprise limited process control, inconsistent syngas quality and composition, and environmental risks like ground water contamination and land subsidence [7]. In addition, low natural gas prices diminish the economic competitiveness of UCG-based H<sub>2</sub> against SMR-based H<sub>2</sub>, especially in western Canada [7].

---

<sup>3</sup> Initial studies have suggested that three coal zones in Alberta – Ardley, Horseshoe Canyon, and upper Mannville – are suitable for UCG. These three zones constitute around 54% of the total coal reserves. Owing to greater depth, upper Mannville (which has around 16% of the total coal reserves) is the most favorable coal zone for UCG in terms of ground water protection and unwanted overburden subsidence [12].

Since coal has the highest CO<sub>2</sub> emissions of all fossil fuels per unit of energy produced, the conversion of syngas to electricity or H<sub>2</sub> produces significant amounts of CO<sub>2</sub> emissions [18, 20, 21]. Carbon capture and sequestration (CCS) technology captures CO<sub>2</sub> using a physical solvent within a pre-combustion arrangement and then stores the CO<sub>2</sub> in an underground geological formation for enhanced oil recovery (EOR) or enhanced coal bed methane (ECBM) recovery [15, 20-22]. Moreover, geological sequestration sites (such as saline aquifers) have been found to co-exist with potential UCG sites [17, 20, 21]. The Western Canadian Sedimentary Basin, in which most of the Alberta's coal reserves are found, has many favorable CO<sub>2</sub> sequestration sites<sup>4</sup> [7]. Interestingly, UCG and CCS can be coupled in a process wherein the captured CO<sub>2</sub> is sequestered into a coal seam cavity created upon gasification by using the same injection and production wells [18, 21]. A similar integrated UCG-CCS process was discussed for a study area in Bulgaria by Nakaten et al. [23]. Admittedly, with huge un-mineable coal reserves in Alberta and with UCG and CCS potential, a low-carbon H<sub>2</sub> production pathway should be analyzed in terms of sustainable development of the bitumen upgrading industry.

There are a few studies in the literature that discuss H<sub>2</sub> production from UCG. Yang et al. [24] discussed the fundamentals of H<sub>2</sub> production by analyzing the experimental conditions and the UCG process in China. Rogut et al. [25] discussed the potential of UCG for large-scale integration of H<sub>2</sub> production with on-site geological storage of CO<sub>2</sub> in the European Union. Some studies have discussed a techno-economic model for electricity and H<sub>2</sub> production from an integrated UCG-CCS process [7, 23]. Nakaten et al. [23] concluded that the UCG-CCS process, integrated with a combined cycle (CC) gas turbine (GT) is an economical, low-carbon option for electricity production in Bulgaria. Prabu et al. [26] developed a model to estimate electrical plant efficiency for an integrated

---

<sup>4</sup> Alberta Carbon Trunk Line, a 40.6 cm, 240 km CO<sub>2</sub> pipeline expected to be operational in 2015, will transport CO<sub>2</sub> collected from current and proposed bitumen upgraders to EOR fields in central and southern Alberta [8].

UCG-solid oxide fuel cell system (SOFC) system. Nourozieh et al. [27] conducted a feasibility study for Alberta reservoirs by developing a simulation model for process optimization and prediction of syngas production. Moreover, Swan Hills Synfuels LP has successfully constructed and operated the world's deepest in-situ coal gasification pilot facility in Alberta [28].

With that said, none of the aforementioned authors developed models that provide a holistic evaluation of the energy balances involved in UCG for H<sub>2</sub> production, along with the integration of CCS technology. This holistic approach is especially important to characterize the energy conversion efficiency of UCG as a H<sub>2</sub> production pathway, which provides insight into its competitiveness with other conventional options. In addition, the resolution of the energy flows in the H<sub>2</sub> production from UCG leads to the identification of energy-intensive centers along with improvements in the overall system management. Furthermore, the results can be applied to evaluate the life cycle GHG emissions, and GHG mitigation potential and costs associated with H<sub>2</sub> production from UCG along with consideration of CCS [29, 30].

The system design of converting H<sub>2</sub> from syngas produced from UCG is identical to that of H<sub>2</sub> produced from SCG [15, 16], and the latter is well understood in various studies [31-42]. Following [31-42], a model to estimate and analyze key performance estimates (coal-to-H<sub>2</sub> conversion efficiency ( $\eta_h$ ) and electrical energy exported to grid per unit coal energy ( $\eta_e$ ) of UCG-based H<sub>2</sub> production can readily be developed. The model is called FUNNEL-EGY-H2-UCG (**FUN**damental **EN**gineering **Principle**s-based **Model** for **E**stimation of **E**ner**GY** consumption and production in hydrogen (**H2**) production from **U**nderground **C**oal **G**asification) in this paper. While these studies [31-42] focused more specifically on mineable coal and natural gas as a feedstock, this paper addresses the gap in knowledge in the area of energy balances and the evaluation of plant efficiency in the production of H<sub>2</sub> from un-mineable coal resources through UCG. Furthermore, this paper provides a framework through which benchmarking of H<sub>2</sub> conversion efficiency from

UCG can be carried out with SCG- and SMR-based H<sub>2</sub> production pathways. FUNNEL-EGY-H<sub>2</sub>-UCG allows the user to estimate the H<sub>2</sub> conversion efficiency for any type of coal and UCG reservoir conditions. That said, in the current analysis, assumptions pertaining to western Canadian conditions are taken into consideration as closely as possible. This paper also establishes the qualitative and quantitative relationships between key UCG process parameters (H<sub>2</sub>O-to-O<sub>2</sub> injection ratio, ground water influx and steam-to-carbon ratio) and plant efficiency. This is completed by analyzing the results for a range of 2-3 for H<sub>2</sub>O-to-O<sub>2</sub> injection ratio, 0-0.4 m<sup>3</sup>/tonne-coal for ground water influx and 2-4 for steam-to-carbon ratio.

The paper is organized in the following fashion. Section 2 outlines the unit operations of H<sub>2</sub> production from UCG with and without CCS and the methodology adopted in the development of the data-intensive Aspen Plus model. The results and discussions of the work carried out are presented in section 3. The conclusions are provided in section 4.

## **2. Methodology**

### *2.1. Plant layout overview and system boundary: H<sub>2</sub> production from UCG with and without CCS*

The H<sub>2</sub> production pathway from UCG is developed for two different plant configurations: with CCS and without CCS. Figure 1 shows all the unit operations involved in the hydrogen production pathway for the two plant configurations. The underground coal seam is

gasified by injecting H<sub>2</sub>O and O<sub>2</sub> via an injection well. Upon gasification, coal produces syngas, which travels through a production well. This syngas is mainly composed of CO, H<sub>2</sub>, CH<sub>4</sub>, CO<sub>2</sub>, and H<sub>2</sub>O. Apart from this, the syngas also contains traces of H<sub>2</sub>S, C<sub>2</sub>H<sub>6</sub>, NH<sub>3</sub>, and higher hydrocarbons. Based on the composition of the syngas, the H<sub>2</sub> production plant scheme can be derived from existing SCG- and SMR-based H<sub>2</sub> production plant schemes. An extensive review of hydrogen production pathways from surface coal gasification and steam methane reforming, provided in [4, 7, 32, 33, 36, 43] was done to determine assumptions for different post-UCG unit operations (see Fig. 1).

The overall system energy flow of the H<sub>2</sub> production pathway is represented by streams shown outside the system boundary (see Fig.1). The boundary start point is the injection of injection of the gasifying agents for UCG, while the termination point is the H<sub>2</sub> export to a demand site via a pipeline. The difference in the two plant schemes is that CCS uses CO<sub>2</sub> compression, transportation, and sequestration and the configuration without CCS does not. It is important to note that both plant configurations are characterized with CO<sub>2</sub> capture using a physical solvent – Selexol. The H<sub>2</sub> production pathway also consists of a co-generation section, which produces electricity and steam to satisfy the requirements of the different unit operations. Additional electricity produced is exported to the grid outside the system boundary

FUNNEL-EGY-H2-UCG calculates coal-to-H<sub>2</sub> conversion efficiency ( $\eta_h$ ) and electrical energy exported to the grid per unit coal energy ( $\eta_e$ ) as per Eq. (1) and Eq. (2), respectively.  $\eta_e$  is indicative of electricity production in addition to H<sub>2</sub> production, and is expressed as a percentage of input coal energy after taking into account the electricity consumption in different unit operations.



**Fig. 1**

## 2.2. $H_2$ production from UCG – An overview of unit operations

2.2.1. *Injection:* This unit operation involves the injection of gasifying agents, mainly oxygen and water, at a pressure of 20 MPa and 14 MPa, respectively [28]. Oxygen with 95% purity is produced by an air separation unit (ASU) at a pressure of 0.1 MPa, which consumes 0.26 kWh of electricity per kg of pure  $O_2$  production [32, 33]. It is assumed that the in situ coal gasification reactor is connected by a pair of wells; an injection well is a 1400 meters deep and is around 1400 meters from a 1400 meter high production well [28]. The well diameter is 11.4 cm [28].

2.2.2. *Underground coal gasification:* The specification of coal used for in situ gasification is shown in Table 1. Due to a lack of production data for hydrogen production from UCG on a large commercial scale for deep coal seams, in situ coal gasification at a small-scale hydrogen production plant was analyzed. In this paper, operational data, mainly type, amount of coal gasified, and injection flow rates of gasifying agents, are taken from a small-scale UCG pilot plant for syngas production operated by Swan Hills Synfuels in Alberta [28]. This pilot project is carried out at a depth of 1400 m, which is one of the deepest of the pilot or commercial UCG projects around the world [19, 28]. Owing to greater coal seam depth, the operating pressure of the UCG reactor in Alberta, Canada ranges from 10 to 12.5 MPa [28, 44]. High operating pressures result in low water influx in the gasification zone of the UCG reactor and high gas losses from the rock formation [15, 16].

The authors in [28] describe a controlled retractable ignition point (CRIP)<sup>5</sup> technique that was used to gasify coal underground. The CRIP technique and high operating pressure result in the production of high quality syngas, low heat losses, and improvement of the overall gasification efficiency [19, 45]. The initial UCG reservoir temperature and pressure are assumed to be 60° C and 11.5 MPa, respectively [27]. Heat loss to the surrounding strata in UCG is difficult to estimate and depends on the properties of the dry rock above the coal seam [15, 19]. Also, the UCG process reaches a heat balance on its own [19]. With that said, a nominal temperature decrease of 100° C in the syngas is assumed in this paper to address the heat losses in the UCG reactor. Another factor that is difficult to estimate in UCG is the rate of ground water influx in gasification, which not only affects the composition of the syngas but also the quality and quantity of the syngas [15, 16]. It is also reported in the literature that the influx water will either be part of the gasification reactions or cool the gases in the reactor [16]. It is assumed in the present analysis that ground water (amounting to 0.4 m<sup>3</sup>/tonne of coal)<sup>6</sup> takes part in the gasification reaction, and its effect on  $\eta_h$ , and  $\eta_e$  is addressed.

**Table 1.**

---

<sup>5</sup> The CRIP technique uses coiled tubing for injection through an injection well that is drilled horizontally until it reaches the foot of a production well. Fresh coal is reached by retracting the coil when the cavity has matured (because of which the syngas quality becomes poor) [19].

<sup>6</sup> A ground water influx rate of 0.4 m<sup>3</sup>/tonne of coal is assumed for stable and continuous gas production [46].

One of the most important considerations in estimating H<sub>2</sub> production from UCG is the composition of the syngas collected from the production well. The process of UCG is similar to surface coal gasification, from a chemical and a thermodynamic perspective [48]. The in situ coal will undergo a series of chemical reactions, namely coal drying, pyrolysis, char gasification, boudouard, steam gasification, hydrogen gasification, CO combustion, gas-steam shift, and methane-steam shift<sup>7</sup> [44, 49]. Coal is characterized in Aspen Plus in the form of products obtained after pyrolysis, that is, char, tar, H<sub>2</sub>S, C<sub>2</sub>H<sub>6</sub>, CO, CH<sub>4</sub>, NH<sub>3</sub>, CO<sub>2</sub>, H<sub>2</sub>, ash, and H<sub>2</sub>O. The mass flow rates of each of these constituents are estimated in a similar fashion as done by the authors of [44], using a mathematical model provided by [50]. The syngas composition is estimated based on the minimization of the Gibbs free energy of the UCG reactor using the Peng-Robinson equation of state in Aspen Plus. The model developed is predicated upon the assumption that the UCG reactor reaches equilibrium with the following: surrounding strata, ground water influx, heat losses and gasifying agents (H<sub>2</sub>O and O<sub>2</sub>) at a given point of time. The UCG process is represented by two RGibbs reactors in Aspen Plus. The second RGibbs reactor accounts for heat losses in the UCG reactor by specifying the assumed temperature decrease of 100° C. However, there are

---

<sup>7</sup> Coal drying: Wetcoal → Drycoal + H<sub>2</sub>O, ΔH<sup>0</sup> = 40 kJ/mole; Pyrolysis: Drycoal → Char + Volatiles, ΔH<sup>0</sup> ~ 0 kJ/mole; Char gasification: C + O<sub>2</sub> →

CO<sub>2</sub>, ΔH<sup>0</sup> = -393 kJ/mole; Steam gasification: C + H<sub>2</sub>O → H<sub>2</sub> + CO, ΔH<sup>0</sup> = +131 kJ/mole; Boudouard: C + CO<sub>2</sub> → 2CO, ΔH<sup>0</sup> = +172 kJ/mole;

Hydrogen gasification: C + 2H<sub>2</sub> → CH<sub>4</sub>, ΔH<sup>0</sup> = -75 kJ/mole; CO combustion: CO + 1/2O<sub>2</sub> → CO<sub>2</sub>, ΔH<sup>0</sup> = -283 kJ/mole; Gas-steam shift: CO + H<sub>2</sub>O ↔

CO<sub>2</sub> + H<sub>2</sub>, ΔH<sup>0</sup> = -41 kJ/mole; Methane-steam shift: CH<sub>4</sub> + H<sub>2</sub>O ↔ CO + 3H<sub>2</sub>, ΔH<sup>0</sup> = +206 kJ/mole

limitations with this methodology. The resolution of syngas losses to the surrounding rocks and dynamic temperature-pressure profile in the in situ coal seam and its effect on the syngas composition are beyond the capacity of the model presented.

The composition of the syngas on a dry molar basis based on 118 tonnes per day of coal extracted by UCG for an H<sub>2</sub>O-to-O<sub>2</sub> injection ratio of 2 and a ground water influx of 0.4 m<sup>3</sup>/tonne of coal is given in Table 2. The composition of the produced gas obtained from the model is consistent with reported values in the literature for a variety of coal, i.e., H<sub>2</sub>: 11-35%; CO: 2-16%; CH<sub>4</sub>: 1-8%; CO<sub>2</sub>: 12-28%; H<sub>2</sub>S: 0.03- 3.5% [19]. Considering the high operating pressures in UCG, there is likely to be considerable CH<sub>4</sub> in the produced gas, unlike in low operating pressures, where the CH<sub>4</sub> percentage is lower than that of gas [28, 44]. This is mainly due to the fact that the hydrogenating gasification reaction ( $C + 2H_2 \rightarrow CH_4$ ) is favorable at a high underground reactor pressure [28, 44].

The product gas is treated with steam to convert CH<sub>4</sub> into water gas (H<sub>2</sub> + CO) in a reforming reactor to improve  $\eta_h$ . This reactor is called a syngas reforming reactor (SRR) in this paper.

**Table 2.**

*2.2.3. Hydrogen sulphide (H<sub>2</sub>S) removal:* Sulphur needs to be removed from the product gas obtained from UCG both for economical operation and to avoid poisoning the catalysts in the reforming reaction of the methane present in the product gas [43]. This is unlike in surface coal gasification plant schemes with CCS, where H<sub>2</sub>S is co-captured with CO<sub>2</sub> downstream of water-gas shift reactions [32,

33, 39, 40]. Additionally, prior to H<sub>2</sub>S removal, the highly pressurized product gas obtained from UCG is expanded in a turbine to around 3 MPa<sup>8</sup> to generate electricity and then cooled to 25° C [43]. The heat extracted from the gas is used to raise the temperature of the sulphur-free gas, which is put into the SRR. The polytropic efficiency of the syngas expander is assumed to be 88% [32]. H<sub>2</sub>S capture is carried out in an absorption tower with dimethyl ether of polyethylene glycol (Selexol) as a solvent and an operation pressure of 3 MPa [32, 33, 36, 43]. The process flow scheme from H<sub>2</sub>S absorption to stripping is derived from [36].

The solubility of CO<sub>2</sub> in Selexol is about 8.93 times less than that of H<sub>2</sub>S [51]. However, the amount of CO<sub>2</sub> absorbed in Selexol is significantly greater than the amount of H<sub>2</sub>S absorbed. This is because of higher mole concentration of CO<sub>2</sub> than of H<sub>2</sub>S in the product gas [32] (see Table 2). Therefore, after stripping H<sub>2</sub>S from Selexol, the solvent is fed to a CO<sub>2</sub> absorption tower downstream of water-gas shift reactors (WGSRs) to capture the CO<sub>2</sub>. Close to 99% of H<sub>2</sub>S is removed from the product gas, which is consistent with the 99% H<sub>2</sub>S removal efficiency reported in the literature [31, 32, 36]. Steam (6 MJ, 0.6 MPa steam per kg of sulphur [32]) required to strip H<sub>2</sub>S from the solvent is produced from a heat recovery steam generator (HRSG) in a co-generation plant. The above assumptions are also valid for plant schemes without CCS. Sulphur is recovered in a Claus plant, which consumes 98 kWh of electricity per tonne of sulphur removed<sup>9</sup> [52]. Additional electricity is required to treat tail gas coming from the Claus plant and is assumed to be 463 kWh per tonne of sulphur removed<sup>8</sup> [52].

---

<sup>8</sup> The pressure value is based on values in the literature of steam methane reforming reaction in H<sub>2</sub> production from natural gas plant schemes [43].

<sup>9, 8</sup> Owing to complexity of the processes involved in the Claus plant, the sulphur recovery and tail gas treatment are not modelled in Aspen Plus.

*2.2.4. Syngas to H<sub>2</sub> conversion:* The sulphur-free and CH<sub>4</sub>-rich syngas is processed in a series of reactors to produce H<sub>2</sub>: a steam reforming reactor (SRR) and high temperature (HT) and low temperature (LT) WGSRs. Table 3 shows all the assumptions pertinent to this unit operation. A steam-to-carbon ratio of 3 is assumed in order to get the maximum H<sub>2</sub> output upon syngas conversion [43]. Carbon flow is calculated based on the molar flow of CH<sub>4</sub> and CO in the UCG produced syngas. The syngas is then converted to H<sub>2</sub> in a series of HT and LT WGSRs. A heat exchanger network is modelled in a simplified fashion to use the heat recovered from the WGSRs to produce HP and LP steam in an HRSG. Purge gas, which is produced after the removal of H<sub>2</sub> downstream of CO<sub>2</sub> removal, is burned to satisfy the heat duty of the SRR.

**Table 3.**

*2.2.5. CO<sub>2</sub> removal and transportation:* To integrate hydrogen production from UCG with CCS, CO<sub>2</sub> is absorbed, removed, and compressed before its transportation to a sequestration site [31, 33, 53]. CO<sub>2</sub> is absorbed using Selexol as a solvent because Selexol consumes less energy than other solvents like methyl diethanolamine (MDEA) [33]. The absorbed CO<sub>2</sub> is then separated in a series of flash chambers and finally compressed to a pressure of 15 MPa in five stages [33, 53]. The solvent also absorbs H<sub>2</sub> in the

absorption tower. Therefore, the solvent coming from the first flash chamber is compressed and recycled back to the absorption tower to avoid loss of H<sub>2</sub> [31]. The pressure drop between the first flash chamber and the absorption tower is achieved with a hydraulic turbine [31]. The work extracted from the hydraulic turbine is then used to satisfy a portion of solvent recycle pump work [31]. Table 4 shows key assumptions employed for this unit operation. In H<sub>2</sub> production without CCS, the advantage of CO<sub>2</sub> removal (see Fig. 2) is appreciated by achieving a higher heating value of purge gas (55.15 MJ/kg) post H<sub>2</sub> separation than a CO<sub>2</sub>-rich purge gas of low heating value (3.15 MJ/kg) when no CO<sub>2</sub> removal takes place [32]. Additionally, the purge gas compression power required in the GT section is likely to be reduced, when CO<sub>2</sub> removal takes place ahead of H<sub>2</sub> separation in PSA.

**Table 4.**

Pipeline is assumed to be the mode of transportation of CO<sub>2</sub> to an enhanced oil recovery site. CO<sub>2</sub> is transported as a liquid, and a distance of 100 km from the CO<sub>2</sub> capture site to an EOR site is taken as the base case. CO<sub>2</sub> has a critical pressure of 7.38 MPa; that is, it behaves as a liquid at pressure values greater than 7.38 MPa [53]. Therefore, CO<sub>2</sub> is compressed to a pressure of 15 MPa by means of a five-stage compressor power train [32, 40, 53, 54]. Table 4 shows the key assumptions pertaining to the CO<sub>2</sub> compressors. With an increase in pressure of the captured CO<sub>2</sub>, the temperature also increases in each stage. Since the operating temperature in the compressor power train is assumed to be 31° C, the temperature of the captured CO<sub>2</sub> is decreased through the heat exchanger after each stage. The heat recovered from the heat exchangers is used in the HRSG section to produce steam.

*2.2.6. H<sub>2</sub> removal and transportation:* For plant schemes with and without CCS, H<sub>2</sub>-rich gas after CO<sub>2</sub> removal is processed in a PSA unit to separate H<sub>2</sub> at an efficiency of 85% [32]. Since PSA processes require an elaborate and independent model for their assessment, the H<sub>2</sub> separation is represented as a simple separation process, with an efficiency of 85% [32, 43]. The remaining gas, known as purge gas, consists of the inseparable H<sub>2</sub> and some CH<sub>4</sub>. A portion of the purge gas is then processed to produce electricity and steam in a co-generation plant, while the other portion is burned to satisfy the heat duty of the SRR. High purity (99.99%) H<sub>2</sub> is delivered at a pressure of 2 MPa from PSA [32]. Pipeline is assumed to be the mode of transportation of H<sub>2</sub> to an oil sands upgrading site. A pipeline length of 100 km is used as the base case for H<sub>2</sub> transportation. Typical hydrogen pipeline operating pressures and diameters range from 1 to 3 MPa and 0.25 to 0.30 m, respectively [55]. Considering the exit H<sub>2</sub> gas pressure from PSA, the average of the range is used for the operating pressure in the present analysis. The efficiency of the H<sub>2</sub> compressor is assumed to be 55% [56]. Considering the small-scale H<sub>2</sub> production from UCG and the transportation of H<sub>2</sub>, a lower value, 0.25 m, is used for pipeline diameter. The compressor power requirement is calculated using the method developed by Ogden [56].

*2.2.7. Co-generation plant:* This section includes several components, mainly gas turbine (GT), HRSG, and steam turbine. The amount of purge gas fed to the burner is calculated based on the amount of heat duty required in the SRR. The remaining purge gas is compressed, combusted, and then expanded in a GT to produce electricity. The amount of air fed to the GT combustor is specified based on a turbine inlet temperature of 1300° C. The HRSG produces high-pressure (HP) and low-pressure (LP) steam from heat

recovered from the SRR and the WGSRs as well as exhaust gas from the GT. The HP steam, at 3 MPa, is fed to the SRR, and the LP steam, at 0.6 MPa, is fed to the H<sub>2</sub>S stripper. Table 5 shows key assumptions employed for this unit operation. The temperature of the exhaust gas is assumed to be 100°C [33]. Based on an average heat exchanger efficiency of 60%; heat losses in heat recovery are assumed to be 40%. Auxiliary power consumption is assumed to be 2% of the gross power output [31, 32]; this makes up for the power consumption in the process and feed-water pumps [32]. Additionally, a transmission loss of 6.5% of net electricity or additional electricity produced is accounted for in estimating  $\eta_e$  (see Eq. (2)) [2].

**Table 5.**

*2.3. Scope of assumptions and model results*

The input data and assumptions used in FUNNEL-EGY-H2-UCG are both generic and site-specific in nature. All the site-specific assumptions are associated with two unit operations – injection and UCG. These input data include coal type, UCG reservoir depth and pressure, and characteristics of injection gasifying agents. These inputs have direct implications on the quality and quantity of the syngas produced that ultimately affects the H<sub>2</sub> conversion efficiency. On the other hand, all the assumptions considered in the unit operations described in sections 2.2.3 – 2.2.7 are generic. In other words, the FUNNEL-EGY-H2-UCG can be used to evaluate H<sub>2</sub> conversion efficiency from any type of UCG coal seam. Based on the above discussion and model assumptions, the energy and

material balance was performed in Aspen Plus. The process flow diagrams and input-output flows associated with each unit process are enclosed in Appendix A of the paper in the Supplementary Section.

### 3. Results and discussion

#### 3.1. Power requirement in different unit operations: $H_2$ production from UCG with and without CCS

Table 6 shows key parameters of FUNNEL-EGY-H<sub>2</sub>-UCG and a detailed breakdown of the total power consumption in producing H<sub>2</sub> from UCG with and without CCS. Based on a coal LHV of 28.5 MJ/kg and input of 118 tonnes/day [28, 47] (see Table 1), the total rate of coal input energy is calculated as 38.92 MW. This value is the same in H<sub>2</sub> production both with and without CCS. The gross power output from the syngas expander, ST and GT, estimated to be 4.23 MW for a steam-to-carbon ratio of 3, is also the same for both plant configurations. The total system power requirement in H<sub>2</sub> production without CCS is less than in H<sub>2</sub> production with CCS; there is a net power output (which is exported to the grid) of 0.93 MW and 1.83 MW in addition to H<sub>2</sub> production with CCS and without CCS, respectively.  $\eta_h$ , which represents the fraction of the coal energy converted to H<sub>2</sub> energy (see Eq. (1)), is calculated as 58.08 % for both plant configurations. Since the net power output is different in the two plant configurations,  $\eta_e$  is estimated to be 2.39% and 4.69% (see Eq. (2) and Table 6) in H<sub>2</sub> production with CCS and without CCS, respectively. Evidently, the increased  $\eta_e$  in the H<sub>2</sub> production plant configuration with no CCS is due to the “no CO<sub>2</sub> compressor” power requirement. This increase of 2.3% in  $\eta_e$  is consistent and can be compared with reported values in the literature for H<sub>2</sub> production from SCG with CO<sub>2</sub> capture [32]. CO<sub>2</sub>

capture efficiency, calculated as 91.6%, is also found to be in close agreement with existing values in various studies and models [2, 31-34, 38, 41].

The benefit of the co-generation is realized in both plant configurations as the H<sub>2</sub> production pathway becomes self-sufficient in terms of steam and heat production (see Table 6). This is attributable to the fact that the FUNNEL-EGY-H<sub>2</sub>-UCG is developed in such a way that the heat and steam requirement in different unit operations matches with the heat and steam production in the co-generation section. The model calculates the steam requirement in the SRR, WGSRs and H<sub>2</sub>S stripper, and appropriate amount of steam is produced in the co-generation section. An increase in steam demand (applicable in a case when a higher steam-to-carbon ratio is assumed) leads to a reduction in electricity output by the ST and vice versa. Moreover, the model calculates the heat requirement in the SRR unit and allocates appropriate amount of purge gas (the main source of heat) to the burner of the SRR, and GT in the co-generation section for electricity production.

**Table 6.**

Figures 2 and 3 show the power distribution in different unit operations of H<sub>2</sub> production from UCG with and without CCS. Injection, which comprises an ASU, O<sub>2</sub> compressor, and water pump, consumes around 33.4% and 47.7% of the total power requirement in H<sub>2</sub> production with and without CCS, respectively. The power requirement in the CO<sub>2</sub> removal is also significant and contributes 35.7%

and 50.9% to the total power consumption in H<sub>2</sub> production with CCS and without CCS, respectively. CO<sub>2</sub> compressors contribute around 29.9% and 0% of the total power requirement in H<sub>2</sub> production with and without CCS, respectively. This zero power requirement in the “no CCS” plant configuration is because there is no CO<sub>2</sub> compression. Only a fraction of the total electricity consumption is taken for H<sub>2</sub> compression and sulphur recovery, with values of approximately 1% in H<sub>2</sub> production with CCS and 1.4% in H<sub>2</sub> production without CCS. Unarguably, with an increase in the scale of operation or pipeline transportation distance, the pipeline configuration may require additional booster stations to overcome the increased friction losses and keep the flow in a liquid state. In that case, the total power requirement is likely to increase. The H<sub>2</sub> compressor requirement in both plant configurations is, however, insignificant compared to other system components’ power requirements. This is mainly because the small-scale H<sub>2</sub> pipeline operation requires less pressure increase in the inlet pipeline booster station in order to maintain the assumed operating pressure of the pipeline. Conversely, for a large-scale H<sub>2</sub> production plant, the power requirement is likely to increase to overcome the increased friction losses in the pipeline.

**Fig. 2**

**Fig. 3**

Figure 4 depicts energy input and energy output associated with different operations in the two H<sub>2</sub> production plant configurations (with and without CCS). The only noticeable difference in the energy balance diagram for the two plant configurations is in the CO<sub>2</sub> compressor requirements, the consequence of which is realized in a higher export of electricity to the grid in H<sub>2</sub> production without CCS than with. The losses, which are the difference of total energy inputs and total energy outputs, are estimated as 16.01 MW and 15.05 MW in H<sub>2</sub> production with and without CCS, respectively.

**Fig. 4**

### *3.2. The effect of the steam-to-carbon ratio on $\eta_h$ and $\eta_e$*

The steam-to-carbon ratio plays an important role in the conversion of syngas into H<sub>2</sub> in an SCG-based H<sub>2</sub> production plant [32]. Chiesa et al. [32] demonstrated that by increasing the steam to carbon from 0.55 to 1.48 in the SCG-based H<sub>2</sub> production plant increases the H<sub>2</sub> production by 26%. Therefore, it becomes equally important to investigate the effect of this parameter in UCG-based H<sub>2</sub> production plant efficiencies. The steam-to-carbon ratio is defined as the ratio of steam molar flow in the SRR and molar flow carbon (in the form of CH<sub>4</sub> and CO) in the UCG-based syngas. Figure 5 shows the effect of the steam-to-carbon ratio on  $\eta_h$  and  $\eta_e$  in H<sub>2</sub> production from UCG with and without CCS. Considering the fact that the ground water influx rate in the UCG reactor is

difficult to estimate, the analysis was done for various ground water influx rates ranging from 0 to 0.4 m<sup>3</sup> per tonne of coal. Carbon molar flow is calculated based on the product gas available from the production well of the UCG plant. For a ground water influx of 0.4 m<sup>3</sup> per tonne of coal, with an increase in the steam-to-carbon ratio from 2 to 4,  $\eta_h$  increases from 51.4% to 62.6%. This is because a higher flow of steam is favorable for converting CH<sub>4</sub> into H<sub>2</sub> in SRR and CO into H<sub>2</sub> in WGSRs, ultimately increasing the net H<sub>2</sub> output. It is important to note that this trend is identical in both plant configurations – H<sub>2</sub> production with and without CCS – because the unit operations and their conditions are the same until H<sub>2</sub> separation and transport (see Fig. 1).

However, there is a counter effect on  $\eta_e$  with an increase in the steam-to-carbon ratio. With an increase in steam flow to the SRR, the unconverted CH<sub>4</sub> concentration decreases, and the CO<sub>2</sub> flow rate increases in the product gas downstream of WGSRs. These increases result in a lower heating value of the purge gas after CO<sub>2</sub> removal and H<sub>2</sub> separation in the PSA and ultimately lower GT power output. Additionally, the amount of heat recovered from the WGSRs decreases with an increase in steam flow, resulting in lower ST power output. Overall, the gross power output decreases with an increase in steam flow. However, the power required to remove and compress CO<sub>2</sub> for sequestration increases because of the increased CO<sub>2</sub> flow rate. Overall, the net power output decreases with an increase in the steam-to-carbon ratio. For a fixed ground water influx rate of 0.4 m<sup>3</sup> per tonne of coal, with an increase in the steam-to-carbon ratio from 2 to 4,  $\eta_e$  decreases from 5.4% to 0.4% in H<sub>2</sub> production with CCS, whereas the decrease in the magnitude of  $\eta_e$  ranges from 7.6% to 2.8% in H<sub>2</sub> production without CCS.

It is interesting to note that for a fixed steam-to-carbon ratio,  $\eta_h$  decreases with an increase in ground water influx in the UCG reactor (see Fig. 5). This stems from the fact that with a rise in ground water influx, the CH<sub>4</sub> content in the syngas obtained from the production well increases, whereas its H<sub>2</sub> content decreases. As a consequence, the steam consumption in the SRR unit rises in

order to maintain the fixed steam to carbon ratio, thus compensating for the shortfall in H<sub>2</sub> content of the syngas. The aggregate effect of this amounts to a slight drop in the H<sub>2</sub> output as shown in Fig. 5. On the other hand, the rise in CH<sub>4</sub> content of the syngas results in a small appreciation in the value of  $\eta_e$ . The reason for this trend is two-fold. First, the increase in CH<sub>4</sub> content of the syngas results in an increase in the total flow of the purge gas. At the same time, due to increased steam consumption, the heat duty requirement in the SRR unit also rises. Since a greater portion of the purge gas is burned in a combustor to satisfy this heat requirement, the flow of the purge gas fed to the GT is only slightly increased. As a result, only a small increase in the GT power output is observed. Second, the rise in the steam consumption imposes a penalty in the power output of the ST.

**Fig. 5**

### *3.3. The effect of H<sub>2</sub>O-to-O<sub>2</sub> injection flow ratio on $\eta_h$ and $\eta_e$*

Stability of the UCG operation in relation to the quality of the syngas can be achieved by controlling the H<sub>2</sub>O-to-O<sub>2</sub> injection ratio [28]. At the same time, the H<sub>2</sub>O-to-O<sub>2</sub> ratio was found to have a significant influence on the product gas composition [27]. Clearly, it is imperative to appreciate and analyze the sensitivities of variable H<sub>2</sub>O-to-O<sub>2</sub> injection ratios on H<sub>2</sub> production from UCG-based syngas. Figure 6 shows the effect of the H<sub>2</sub>O-to-O<sub>2</sub> injection ratio on  $\eta_h$  and  $\eta_e$  in H<sub>2</sub> production from UCG with and without CCS. Again, due to the uncertainty of the ground water influx in the UCG reactor, the sensitivity of the H<sub>2</sub>O-to-O<sub>2</sub> ratio for different influx

rates is investigated. For the same reasons mentioned in the above section,  $\eta_h$  increases as ground water influx increases. Other parameters remain the same. At the same time, the effect of ground water influx on  $\eta_e$  is negligible.

However, with an increase in H<sub>2</sub>O-to-O<sub>2</sub> ratio,  $\eta_h$  decreases. This is mainly due to an increase in CH<sub>4</sub> content and a decrease in H<sub>2</sub> content in the product gas after UCG, resulting in a lower H<sub>2</sub> flow rate for the same flow rate of steam in the SRR and the WGSRs. The findings of the effect of the H<sub>2</sub>O-to-O<sub>2</sub> ratio on the product gas composition provided by the present model – FUNNEL-EGY-H2-UCG – are found to be consistent with a simulation study done for a similar type and depth of in situ coal gasification by the authors in [27]. Overall, the  $\eta_h$  decreases from 58.1% to 54.4% as the H<sub>2</sub>O-to-O<sub>2</sub> ratio is increased from 2 to 3 for a fixed ground water influx rate of 0.4 m<sup>3</sup> per tonne of coal. Contrastingly,  $\eta_e$  increases marginally with an increase in the H<sub>2</sub>O-to-O<sub>2</sub> ratio, with values ranging from 2.1% to 3.1% and 4.4% to 5.4% for a range of ground water influx rates (0 to 0.4 m<sup>3</sup> per tonne of coal) in H<sub>2</sub> production with and without CCS, respectively. This counter effect is justified by a slight increase in net power output by the GT due to an increase in the CH<sub>4</sub> flow in the purge gas on increase in the H<sub>2</sub>O-to-O<sub>2</sub> injection ratio.

**Fig. 6**

### 3.4. Sensitivity analysis

Figure 7 depicts the sensitivity analysis done for H<sub>2</sub> production from UCG with CCS, wherein the ground water influx rate is 0.4 m<sup>3</sup> per tonne of coal and the H<sub>2</sub>O-to-O<sub>2</sub> ratio is 2. It is important to mention that the same trend is observed when the analysis is conducted for H<sub>2</sub> production without CCS; the only difference is in the absolute values of electrical efficiencies because there is no CO<sub>2</sub> compressor power requirement in this plant configuration.

$\eta_h$  is most sensitive to H<sub>2</sub> separation efficiency in the PSA unit. A 10% reduction in the H<sub>2</sub> separation efficiency would result in a decrease of  $\eta_h$  from 58.1% to 52.3 %, while  $\eta_e$  would increase from 2.4% to 4.4% because of increased GT power output.

Conversely, a 10% increase in the H<sub>2</sub> separation efficiency would result in a rise of  $\eta_h$  from 58.1% to 63.9% and a decline in  $\eta_e$  from 2.4% to 0.4%. All the other variables, namely heat exchanger efficiency, GT inlet temperature and pressure ratio, CO<sub>2</sub> compressor isentropic efficiency, and H<sub>2</sub> and CO<sub>2</sub> pipeline transportation distance, have no effect on  $\eta_h$ . However, a temperature decrease in the UCG reactor has a marginal effect on  $\eta_h$ . The greater the temperature decrease in the UCG reactor, the lower the  $\eta_h$ . This is mainly because of increased CH<sub>4</sub> content in the produced gas after the UCG process [19, 46].

The sensitivity of the heat exchanger efficiency on  $\eta_e$  can be appreciated; because of an increase in total heat available in the HRSG, steam production increases, ultimately resulting in increased ST power output, and vice-versa.  $\eta_e$  increases from 2.4% to 4.2% with a 20% increase in heat exchanger efficiency. Conversely,  $\eta_e$  decreases from 2.4% to 0.9% with a 20% decrease in heat exchanger efficiency. A moderate non-linear increasing trend is observed for  $\eta_e$  with an increase in the GT inlet temperature. This is mainly because of the non-linear relationship between the GT inlet temperature and the power delivered by the GT. All the other parameters have a marginal effect on  $\eta_e$ .

**Fig. 7**

### *3.5. Electricity production from UCG with and without CCS*

The present analysis illustrates the use of product gas obtained from the UCG process for H<sub>2</sub> production with and without CCS. Taking into account the immaturity of large commercial-scale UCG technology, the literature on the UCG product gas processing for a variety of end uses, i.e., electricity production, H<sub>2</sub> production, etc., is, therefore, limited. However, the authors in [14, 23, 57] predict  $\eta_e$  from a combined UCG-IGCC plant producing only electricity in a range of 36.3% to 43% without carbon capture and 28.8% to 30% with carbon capture. Prabu et al. [26] estimated a net coal-to-electricity efficiency of 32.3 % for an integrated UCG-SOFC-CCS plant. But none of these studies evaluates  $\eta_h$ . If the same set of assumptions employed in this paper is applied, and the PSA unit is removed from the H<sub>2</sub> production pathway, it becomes easy to derive a plant configuration that produces only electricity from the produced syngas of the UCG process. The electrical efficiency in plants producing only electricity is evaluated to be 32.1% with CCS and 38% without CCS. The results from this plant configuration are found to be in close agreement with the numbers reported in existing studies. The decrease of 5.9% in the electrical efficiency for adopting a CCS plant configuration against a non-CCS plant configuration is also found to be consistent with the value of 6% reported in [23]. This analysis validates the practicality of the

FUNNEL-EGY-H2-UCG presented in the paper under the stated set of assumptions for different unit operations of the H<sub>2</sub> production pathway.

### *3.6. Comparative analysis: H<sub>2</sub> production from UCG vs SCG vs SMR*

In a carbon constrained economy such as western Canada's, where the focus is to move towards clean energy for GHG mitigation, it is important to evaluate the competitiveness of a technology (UCG combined with CCS) that has the potential to recover un-mineable coal and reduce the overall carbon footprint for H<sub>2</sub> production. Table 7 shows typical H<sub>2</sub> plant efficiencies in fossil-fuel based H<sub>2</sub> production pathways (SCG, SMR, and UCG with and without CCS) derived from various studies. Carbon capture technology in most of the listed studies is through physical absorption by Selexol and amines for surface coal gasification and SMR, respectively. The competitiveness of H<sub>2</sub> production of UCG over SCG can be appreciated, given that  $\eta_h$  in UCG ranges from 51.4% to 65.8% versus a range of 44.5% to 69% in SCG [2, 32, 34, 35, 38, 41]. It is evident from the table that there is also a wide range of  $\eta_h$  – 61% to 73% in H<sub>2</sub> production from SMR [34, 37, 42]. Unarguably, a wide range of efficiency values of H<sub>2</sub> production from SCG and SMR may be attributed to the disparity in the assumptions and the methodology adopted by the authors in the respective studies. Considering the complexity of the H<sub>2</sub> production pathway and the lack of detail in the various studies, it is difficult to outline and justify the dissimilarities that lead to variable outputs [32].

With regard to CO<sub>2</sub> capture efficiency, the value varies from 86.8% to 92% and 85% to 90% for H<sub>2</sub> production from surface coal gasification and SMR, respectively. The CO<sub>2</sub> capture efficiency estimated from the current model of H<sub>2</sub> production from UCG

(FUNNEL-EGY-H2-UCG) – 87% to 95.7% – is in close agreement with the values evaluated in various studies for other H<sub>2</sub> production pathways listed in Table 7. Another observation that can be made for H<sub>2</sub> production from surface coal gasification with CCS is the trade-off between H<sub>2</sub> conversion efficiency, and electrical energy exported per unit coal energy. The higher the H<sub>2</sub> conversion efficiency, the lower the electricity export per unit coal energy. This trend is also true for H<sub>2</sub> production from UCG (see Figs. 5 and 6).

**Table 7.**

#### **4. Conclusion**

This research provides insight on the energy balances involved in hydrogen production from UCG with and without CCS. In particular, the authors have developed the relationship between key process variables and hydrogen conversion efficiency ( $\eta_h$ ) and electrical energy exported per unit coal energy ( $\eta_e$ ). For base case assumptions,  $\eta_h$  is calculated to be 58.1% for both plant configurations. In addition to H<sub>2</sub> production, around 2.4% and 4.7% of the coal energy is converted to electricity in H<sub>2</sub> production with and without CCS, respectively. The effect of ground water influx on both  $\eta_h$  and  $\eta_e$  is small. Furthermore, the hydrogen conversion efficiency falls with a rise in the H<sub>2</sub>O-to-O<sub>2</sub> injection ratio and increases with an increase in steam-to-carbon ratio. An opposite trend is

observed for  $\eta_e$ , where an appreciation of its value occurs with a rise in the injection ratio. However, a decrease in the value of  $\eta_e$  is observed with an increase in steam-to-carbon ratio. In addition, the sensitivity analysis showed that  $\eta_e$  is most sensitive to the efficiency of the heat exchanger and the separation efficiency of the PSA.

### **Acknowledgments**

The authors would like to take this opportunity to acknowledge the NSERC/Cenovus/Alberta Innovates Associate Industrial Research Chair Program in Energy and Environmental Systems Engineering and the Cenovus Energy Endowed Chair Program in Environmental Engineering for providing financial support for the research project. The authors are thankful to Astrid Blodgett for editorial support.

**Supplementary information document.**

## References

- [1] Canadian Association of Petroleum Producers (CAPP). Crude oil: forecasts, markets and transportation. Available at: <http://www.capp.ca/getdoc.aspx?DocId=247759&DT=NTV>. June 2014.
- [2] Wang M. GREET, Model 4.02a; Argonne National Laboratory, U.S. Department of Energy. 2012.
- [3] Cetinkaya E, Dincer I, Naterer GF. Life cycle assessment of various hydrogen production methods. *International Journal of Hydrogen Energy*. 2012;37(3):2071-80.
- [4] Dufour J, Serrano DP, Gálvez JL, González A, Soria E, Fierro JLG. Life cycle assessment of alternatives for hydrogen production from renewable and fossil sources. *International Journal of Hydrogen Energy*. 2012;37(2):1173-83.
- [5] Granovskii M, Dincer I, Rosen MA. Exergetic life cycle assessment of hydrogen production from renewables. *Journal of Power Sources*. 2007;167(2):461-71.
- [6] Spath P, Mann M. Life Cycle Assessment of Hydrogen Production via Natural Gas Steam Reforming. NREL/TP-570-27637; 2005.
- [7] Olateju B, Kumar A. Techno-economic assessment of hydrogen production from underground coal gasification (UCG) in Western Canada with carbon capture and sequestration (CCS) for upgrading bitumen from oil sands. *Applied Energy*. 2013;111(0):428-40.
- [8] Cole S, Itani S. The Alberta Carbon Trunk Line and the Benefits of CO<sub>2</sub>. *Energy Procedia*. 2013;37(0):6133-9.
- [9] Alberta Government. Alberta's Clean Energy Future. Climate Change. Available at: [http://www.oilsands.alberta.ca/FactSheets/CChange\\_FSht\\_Sep\\_2013\\_Online.pdf](http://www.oilsands.alberta.ca/FactSheets/CChange_FSht_Sep_2013_Online.pdf). 2013.

- [10] Beaton A, Langenberg W, Pană C. Coalbed methane resources and reservoir characteristics from the Alberta Plains, Canada. *International Journal of Coal Geology*. 2006;65(1–2):93-113.
- [11] Beaton A, Pana C, Chen D, Wynne D, Langenberg CW. Coalbed methane potential of Upper Cretaceous- Tertiary strata, Alberta Plains. Alberta Energy and Utilities Board, EUB/AGS Earth Sciences Report 2002-06. 2002.
- [12] Richardson RJ. Alberta's 2 Trillion Tonnes Of 'Unrecognized' Coal. Available at: [eipa.alberta.ca/media/43006/alberta\\_2\\_trillion\\_tonnes\\_coal.pdf](http://eipa.alberta.ca/media/43006/alberta_2_trillion_tonnes_coal.pdf). 2010.
- [13] Energy Resources Conservation Board. Alberta's energy reserves 2008 and supply/demand outlook 2009–2017. Available at: <http://www.aer.ca/documents/sts/ST98/st98-2009.pdf>. 2009.
- [14] Pana C. Review of Underground Coal Gasification with Reference to Alberta's Potential. Energy Resources Conservation Board. Alberta Geological Survey. 2009.
- [15] Burton E, Friedmann J, Upadhye R. Best practices in underground coal gasification. Contract W-7405-Eng-48. Livermore, CA: Lawrence Livermore National Laboratory. 2006.
- [16] Gregg DW, Edgar TF. Underground coal gasification. *AIChE Journal*. 1978;24(5):753-81.
- [17] Friedmann SJ, Upadhye R, Kong F-M. Prospects for underground coal gasification in carbon-constrained world. *Energy Procedia*. 2009;1(1):4551-7.
- [18] Khadse A, Qayyumi M, Mahajani S, Aghalayam P. Underground coal gasification: A new clean coal utilization technique for India. *Energy*. 2007;32(11):2061-71.

- [19] Bhutto AW, Bazmi AA, Zahedi G. Underground coal gasification: From fundamentals to applications. *Progress in Energy and Combustion Science*. 2013;39(1):189-214.
- [20] Roddy DJ, Younger PL. Underground coal gasification with CCS: a pathway to decarbonising industry. *Energy & Environmental Science*. 2010;3(4):400-7.
- [21] Self S, Reddy B, Rosen M. Review of underground coal gasification technologies and carbon capture. *International Journal of Energy and Environmental Engineering*. 2012;3(1):1-8.
- [22] Khoo HH, Tan RBH. Life cycle investigation of CO<sub>2</sub> recovery and sequestration. *Environmental Science and Technology*. 2006;40(12):4016-24.
- [23] Nakaten N, Schlüter R, Azzam R, Kempka T. Development of a techno-economic model for dynamic calculation of cost of electricity, energy demand and CO<sub>2</sub> emissions of an integrated UCG–CCS process. *Energy*. 2014;66(0):779-90.
- [24] Yang L, Zhang X, Liu S, Yu L, Zhang W. Field test of large-scale hydrogen manufacturing from underground coal gasification (UCG). *International Journal of Hydrogen Energy*. 2008;33(4):1275-85.
- [25] Rogut J, Steen M. Hydrogen oriented underground gasification of coal. 25th Annual International Pittsburgh Coal Conference, PCC - Proceedings. 2008;2:873-80
- [26] Prabu V, Jayanti S. Integration of underground coal gasification with a solid oxide fuel cell system for clean coal utilization. *International Journal of Hydrogen Energy*. 2012;37(2):1677-88.
- [27] Nourozieh H, Kariznovi M, Chen Z, Abedi J. Simulation Study of Underground Coal Gasification in Alberta Reservoirs: Geological Structure and Process Modeling. *Energy Fuels*. 2010;24:3540–50.

[28] Swan Hills SynFuels. Swan Hills In-Situ Coal Gasification Technology Development. Final Outcomes Report. Prepared for: Alberta Innovates – Energy and Environment Solutions. Available at: [http://www.ai-ees.ca/media/6876/swan\\_hills.pdf](http://www.ai-ees.ca/media/6876/swan_hills.pdf) 2012.

[29] Verma A, Kumar A. Life cycle assessment of hydrogen production from underground coal gasification. *Applied Energy*. 2015;147(0):556-68.

[30] Verma A, Olateju B, Kumar A. Greenhouse gas abatement costs of hydrogen production from underground coal gasification. *Energy*. 2015;85(0):556-68.

[31] Chiesa P, Consonni S. Shift reactors and physical absorption for low-CO<sub>2</sub> emission IGCCs. *J Eng Gas Turb Power*. 1999;121:295-305.

[32] Chiesa P, Consonni S, Kreutz T, Robert W. Co-production of hydrogen, electricity and CO<sub>2</sub> from coal with commercially ready technology. Part A: Performance and emissions. *International Journal of Hydrogen Energy*. 2005;30(7):747-67.

[33] Cormos C-C. Integrated assessment of IGCC power generation technology with carbon capture and storage (CCS). *Energy*. 2012;42(1):434-45.

[34] Damen K, Troost Mv, Faaij A, Turkenburg W. A comparison of electricity and hydrogen production systems with CO<sub>2</sub> capture and storage. Part A: Review and selection of promising conversion and capture technologies. *Progress in Energy and Combustion Science*. 2006;32(2):215-46.

[35] Doctor RD, Molburg JC, Chess KL, Brockmeier NF, Thimmapuram PR. Hydrogen production and CO<sub>2</sub> recovery, transport and use from a KRW oxygen-blown gasification combined-cycle system. Argonne National Laboratory draft report, May 1999.

- [36] Doctor RD , Molburg JC , Thimmapuram PR KRW Oxygen-Blown Gasification Combined Cycle: Carbon Dioxide Recovery, Transport, and Disposal. Energy Systems Division, Argonne National Laboratory. ANL/ESD-34. 1996.
- [37] G.H.G. IEA. Decarbonisation of fossil fuels. International Energy Agency Greenhouse Gas R&D Programme, Cheltenham. 1996.
- [38] Klett MG, White JS, Schoff RL, Buchanan TL. Hydrogen production facilities. Plant performance and cost comparisons. Prepared for US DOE/NETL under subcontract 990700362, Task 50802 by Parsons Infrastructure and Technology Group Inc, 2002.
- [39] Li M, Rao AD, Scott Samuelsen G. Performance and costs of advanced sustainable central power plants with CCS and H<sub>2</sub> co-production. Applied Energy. 2012;91(1):43-50.
- [40] Mansouri Majoumerd M, De S, Assadi M, Breuhaus P. An EU initiative for future generation of IGCC power plants using hydrogen-rich syngas: Simulation results for the baseline configuration. Applied Energy. 2012;99(0):280-90.
- [41] National Research Council. The hydrogen economy. Opportunities, costs, barriers, and R&D needs. National Academic Press, Washington 2004.
- [42] Simbeck DR. Hydrogen costs with CO<sub>2</sub> capture. Seventh international conference on greenhouse gas control technologies, Vancouver, Canada. 2004.
- [43] Molburg JC, Doctor RC. Hydrogen from steam-methane reforming with CO<sub>2</sub> capture. Argonne National Laboratory. Available at: <http://seca.doe.gov/technologies/ccbt/refshef/papers/pgh/hydrogen%20from%20steam%20methane%20reforming%20for%20carbon%20dioxide%20cap.pdf>; June 2003.
- [44] Kariznovi M, Nourozieh H, Abedi J, Chen Z. Simulation study and kinetic parameter estimation of underground coal gasification in Alberta reservoirs. Chemical Engineering Research and Design. 2013;91(3):464-76.

- [45] Thorsness CB, Hill RW, Britten JA. Execution and performance of the CRIP process during the rocky mountain I UCG field test. Contract No.: UCRL-98641. Berkeley, CA: Lawrence Livermore National Laboratory (LLNL).1988.
- [46] Yang LH. A Review of the Factors Influencing the Physicochemical Characteristics of Underground Coal Gasification. Energy Sources, Part A: Recovery, Utilization, and Environmental Effects. 2008;30(11):1038-49.
- [47] Smith G, Cameron A, Bustin R. Coal resources of the western Canadian sedimentary Basin. Geological Atlas of the Western Canada Sedimentary Basin. Alberta Geological Survey. Available at:  
[http://www.ags.gov.ab.ca/publications/SPE/PDF/SPE\\_004/chapter\\_33.pdf](http://www.ags.gov.ab.ca/publications/SPE/PDF/SPE_004/chapter_33.pdf).
- [48] Stańczyk K, Kapusta K, Wiatowski M, Świądrowski J, Smoliński A, Rogut J, et al. Experimental simulation of hard coal underground gasification for hydrogen production. Fuel. 2012;91(1):40-50.
- [49] Seifi M, Chen Z, Abedi J. Numerical simulation of underground coal gasification using the CRIP method. The Canadian Journal of Chemical Engineering. 2011;89(6):1528-35.
- [50] Merrick D. Mathematical models of the thermal decomposition of coal: 1. The evolution of volatile matter. Fuel. 1983;62(5):534-9.
- [51] Bucklin RW, Schendel RL. Comparison of Fluor Solvent and Selexol process. Energy progress. 1984;4(3):137-42.
- [52] Abella JP, Bergerson JA. Model to Investigate Energy and Greenhouse Gas Emissions Implications of Refining Petroleum: Impacts of Crude Quality and Refinery Configuration. Environmental Science & Technology. 2012;46(24):13037-47.
- [53] McCollum DL, Ogden JM. Techno-economic models for carbon dioxide compression, transport and storage & correlations for estimating carbon dioxide density and viscosity. Institute of Transportation Studies, University of California, Davis (2006).

- [54] Hertwich EG, Aaberg M, Singh B, Strømman AH. Life-cycle Assessment of Carbon Dioxide Capture for Enhanced Oil Recovery. Chinese Journal of Chemical Engineering. 2008;16(3):343-53.
- [55] Amos WA. Costs of Storing and Transporting Hydrogen. National Renewable Energy Laboratory. NREL/TP-570-25106. 1998.
- [56] Ogden JM. Conceptual Design of Optimized Fossil Energy Systems with Capture and Sequestration of Carbon Dioxide; DOE Award Number: DE-FC26-02NT41623. 2004.
- [57] Nakaten N, Kötting P, Azzam R, Kempka T. Underground Coal Gasification and CO<sub>2</sub> Storage Support Bulgaria's Low Carbon Energy Supply. Energy Procedia. 2013;40(0):212-21.

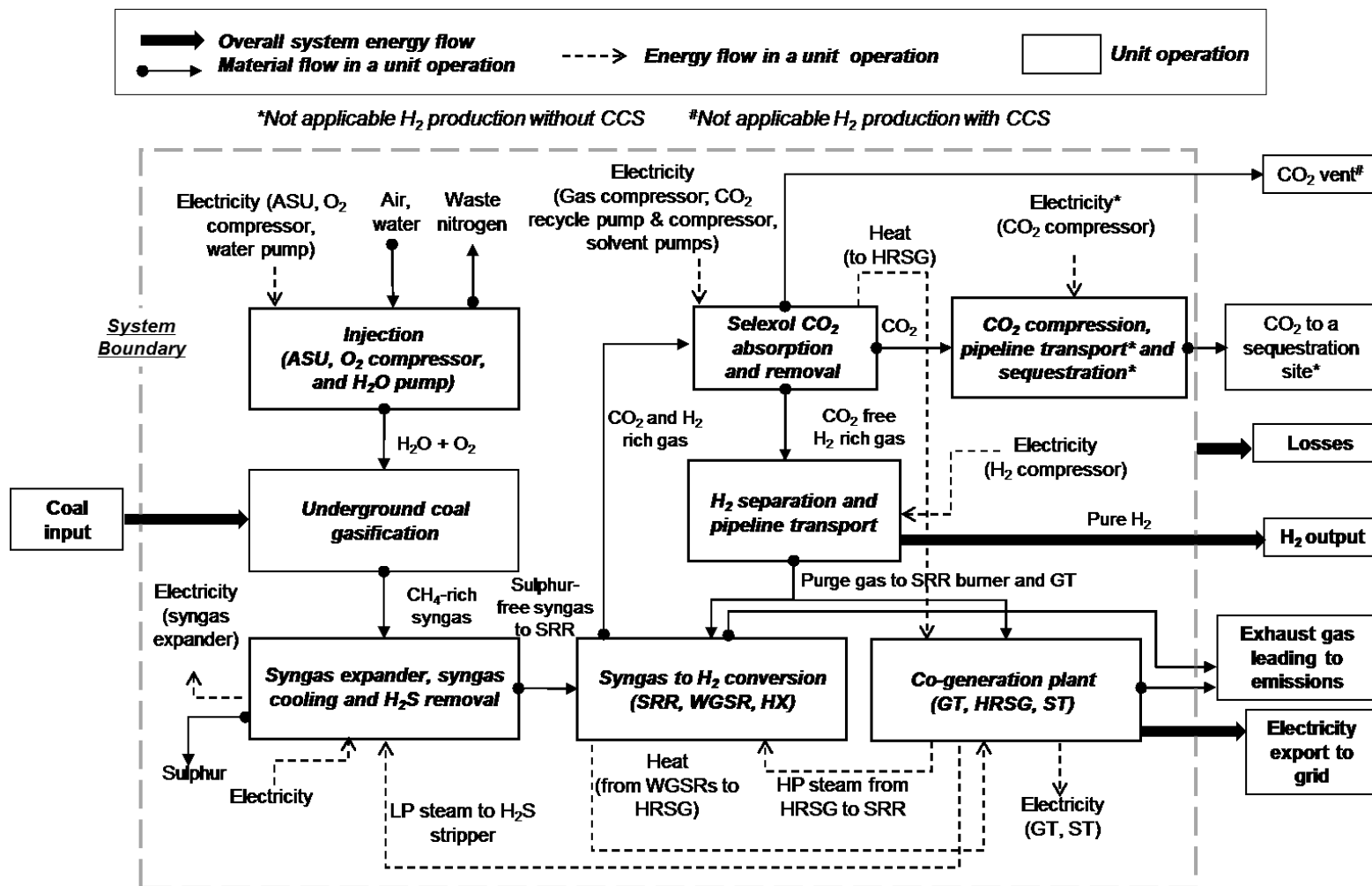


Fig. 1: Unit operations and system boundary of H<sub>2</sub> production pathways from UCG with CCS and without CCS. All unit operations, except O<sub>2</sub> production in ASU, H<sub>2</sub> separation in PSA and sulphur recovery in Claus unit are modelled in Aspen Plus. Notes: ASU-air separation unit; SRR-syngas reforming reactor; WGSR-water gas shift reactor; HX-heat exchanger; GT-gas turbine; HRSG-heat recovery steam generator; ST-steam turbine.



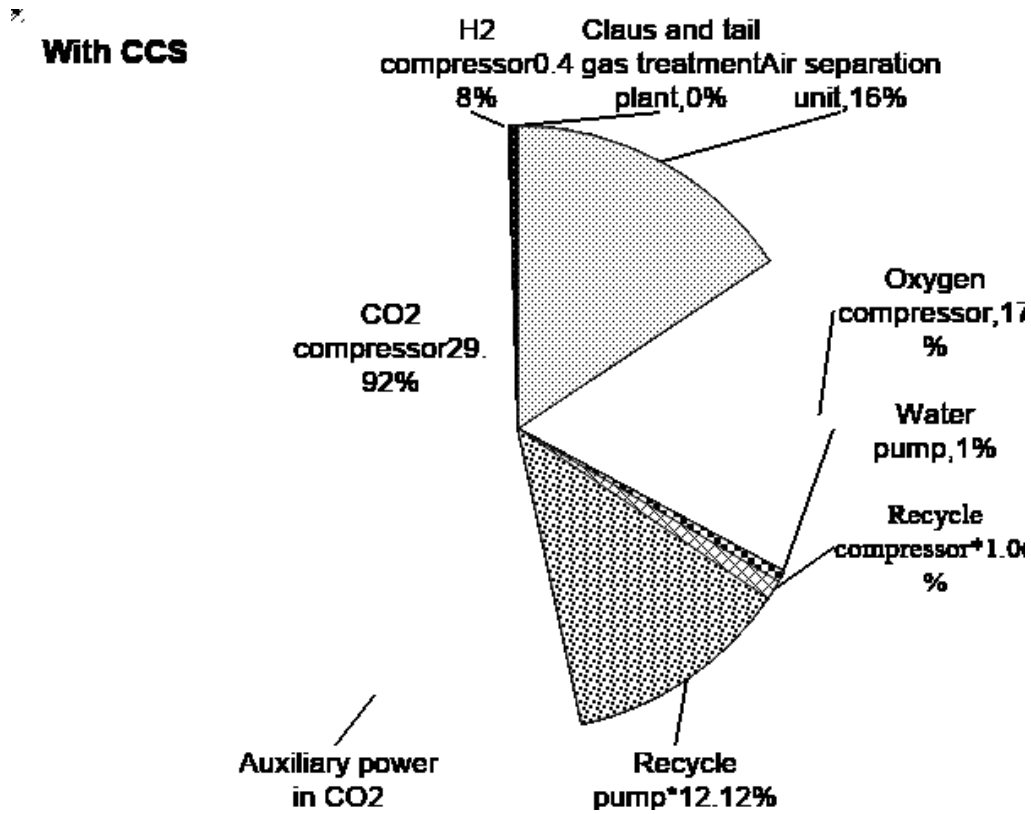


Fig. 2: Power distribution for H<sub>2</sub> production from UCG with CCS

\*Applies to the CO<sub>2</sub> removal section

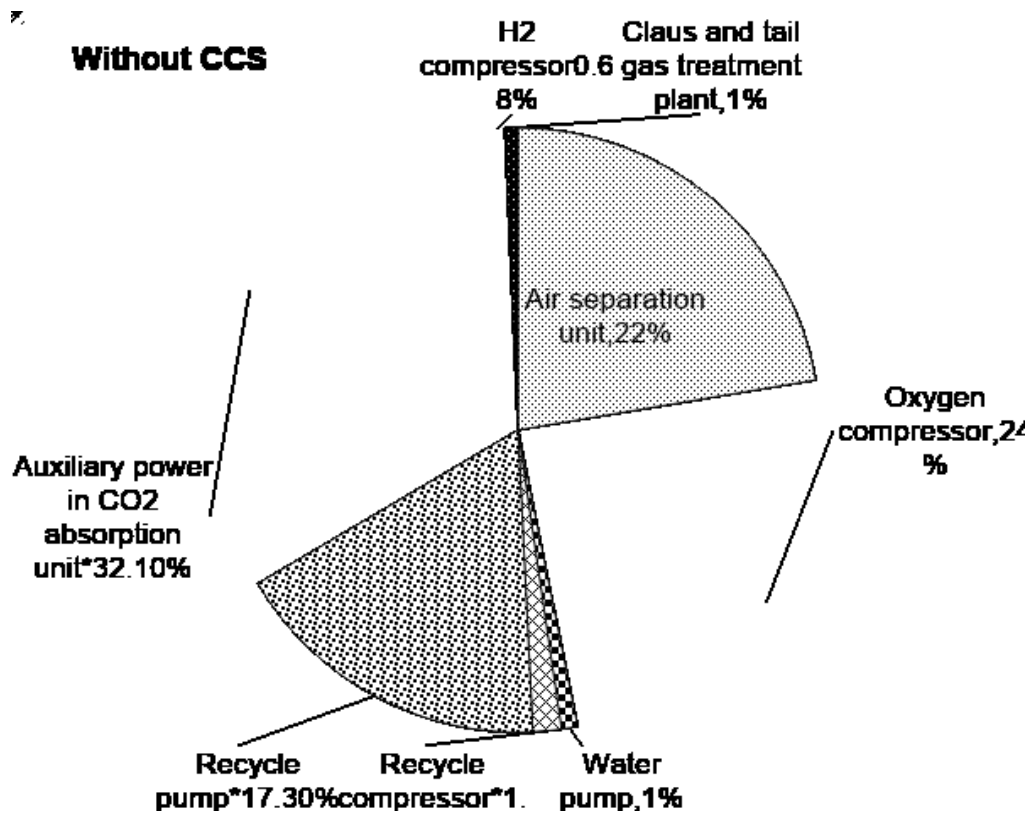


Fig. 3: Power distribution for H<sub>2</sub> production from UCG without CCS

\*Applies to the CO<sub>2</sub> removal section

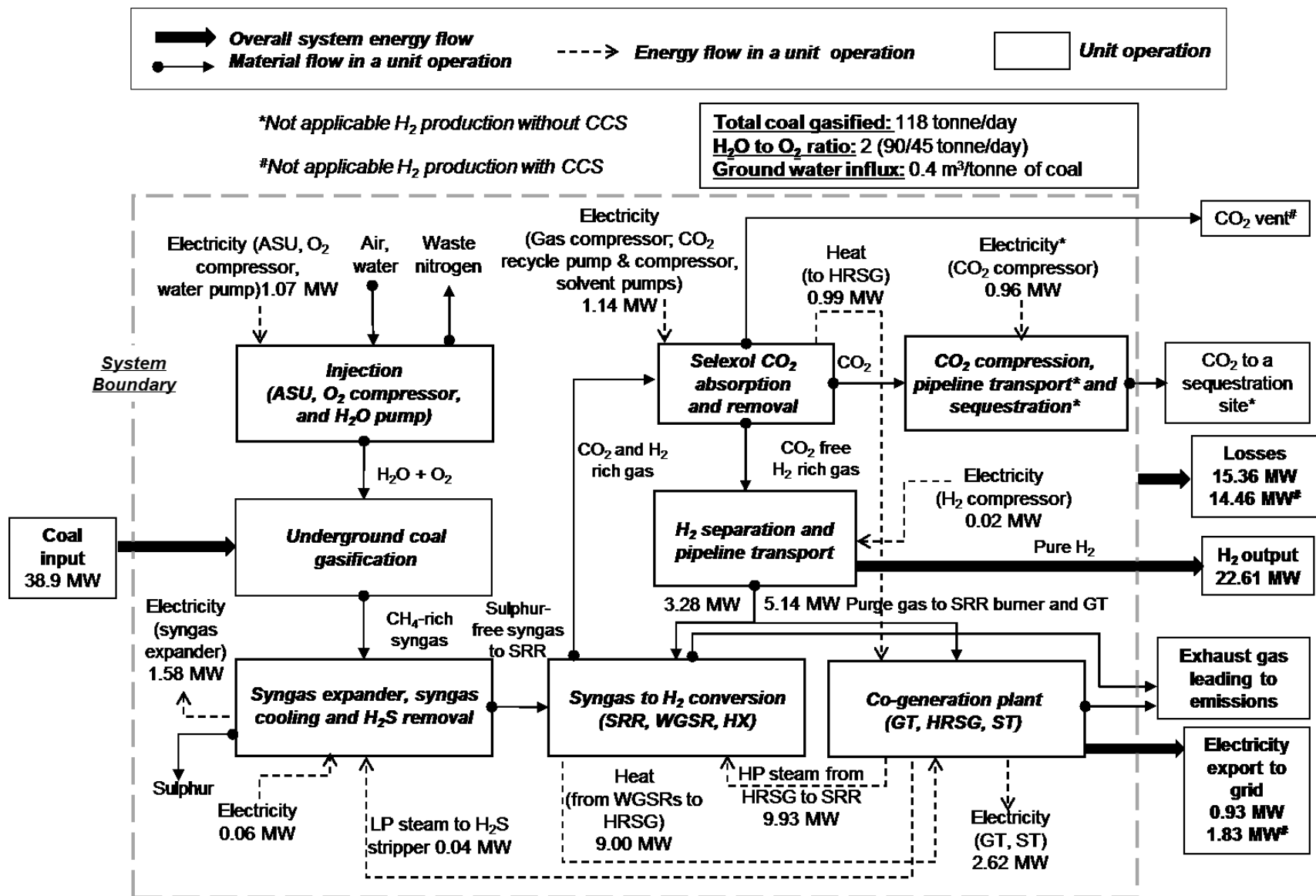
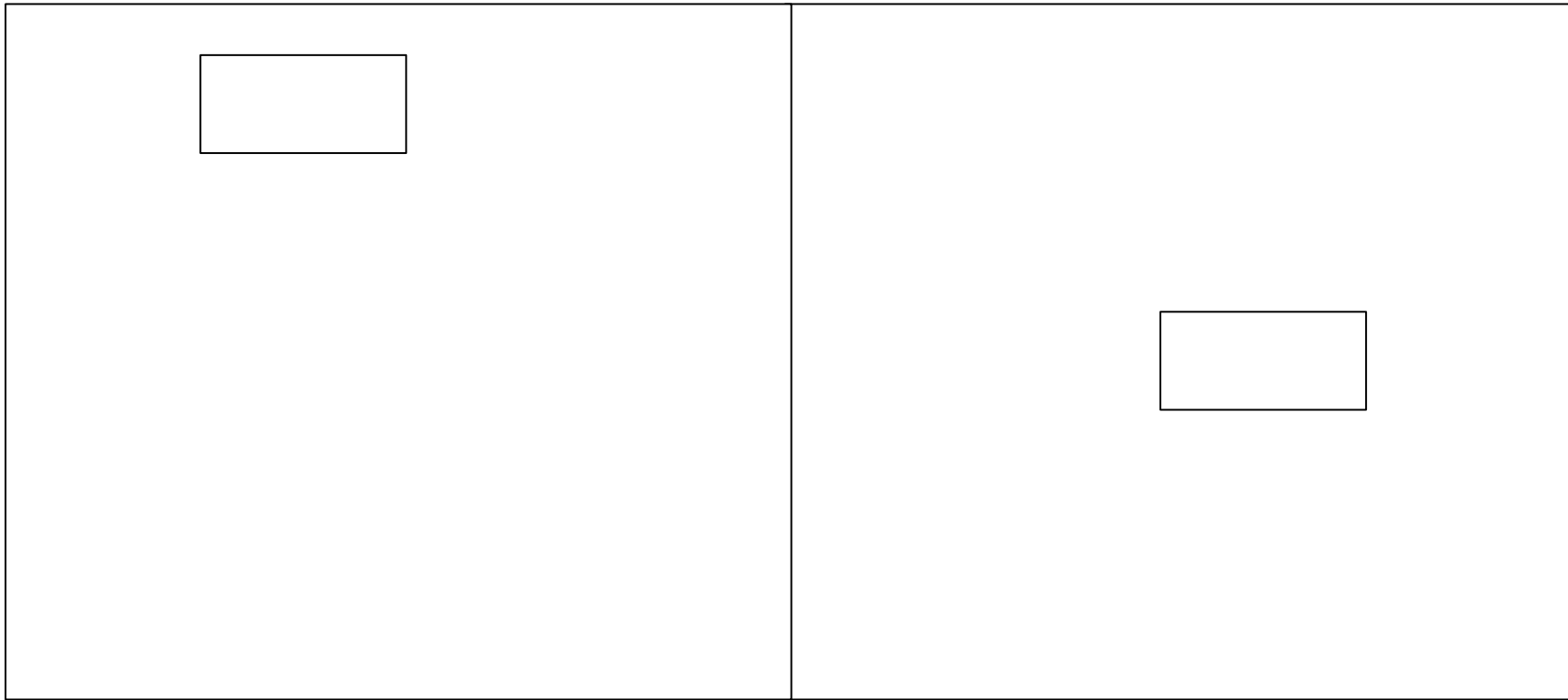


Fig. 4: Energy balance diagram: H<sub>2</sub> production from UCG with and without CCS





**Fig. 5: The effect of the steam-to-carbon ratio on  $\eta_h$  and  $\eta_e$  in  $H_2$  production from UCG with CCS with different ground water influx rates and a fixed  $H_2O$ -to- $O_2$  injection ratio of 2. Dash lines represent  $\eta_h$  and solid lines represent  $\eta_e$**



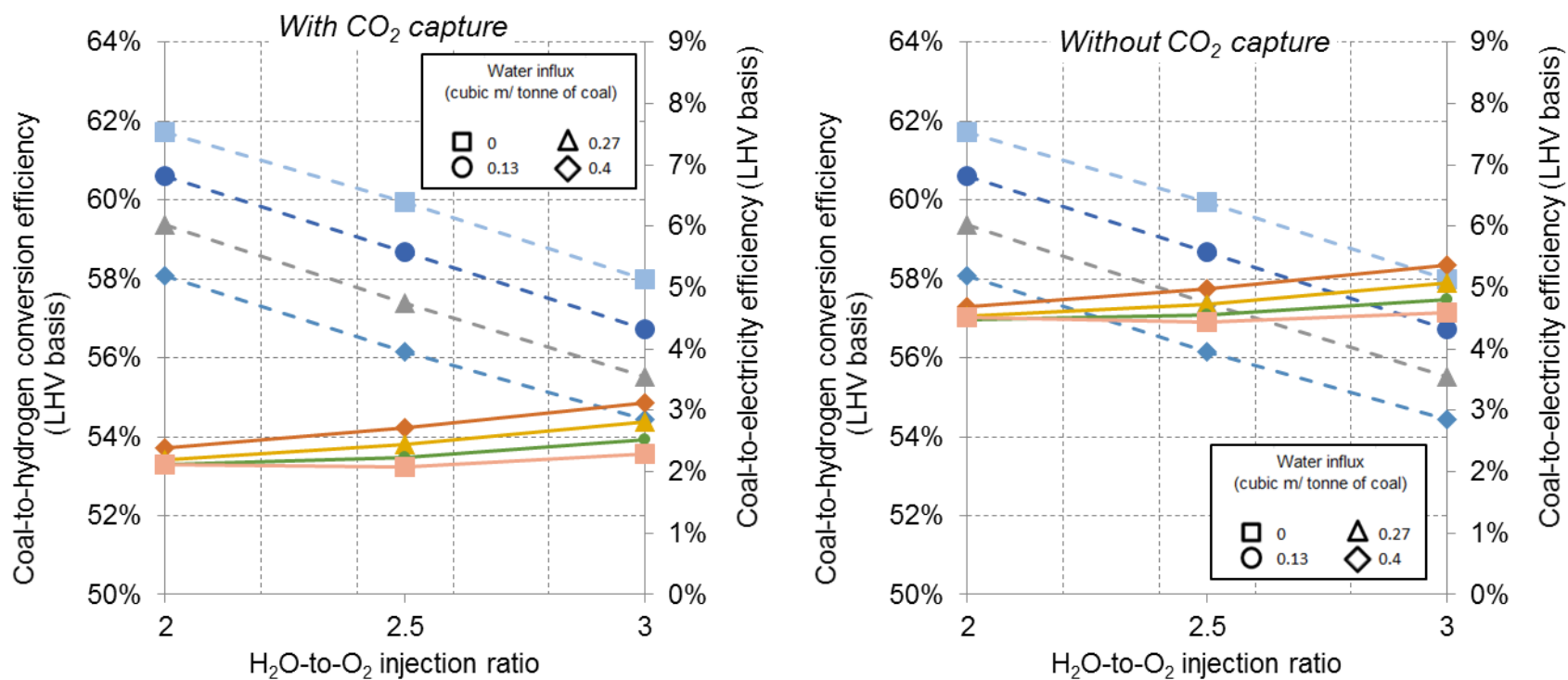


**Fig. 6: The effect of the H<sub>2</sub>O-to-O<sub>2</sub> injection ratio on  $\eta_h$  and  $\eta_e$  in H<sub>2</sub> production from UCG with CCS with different ground water influx rates and a fixed steam-to-carbon ratio of 3. Dash lines represent  $\eta_h$  and solid lines represent  $\eta_e$**

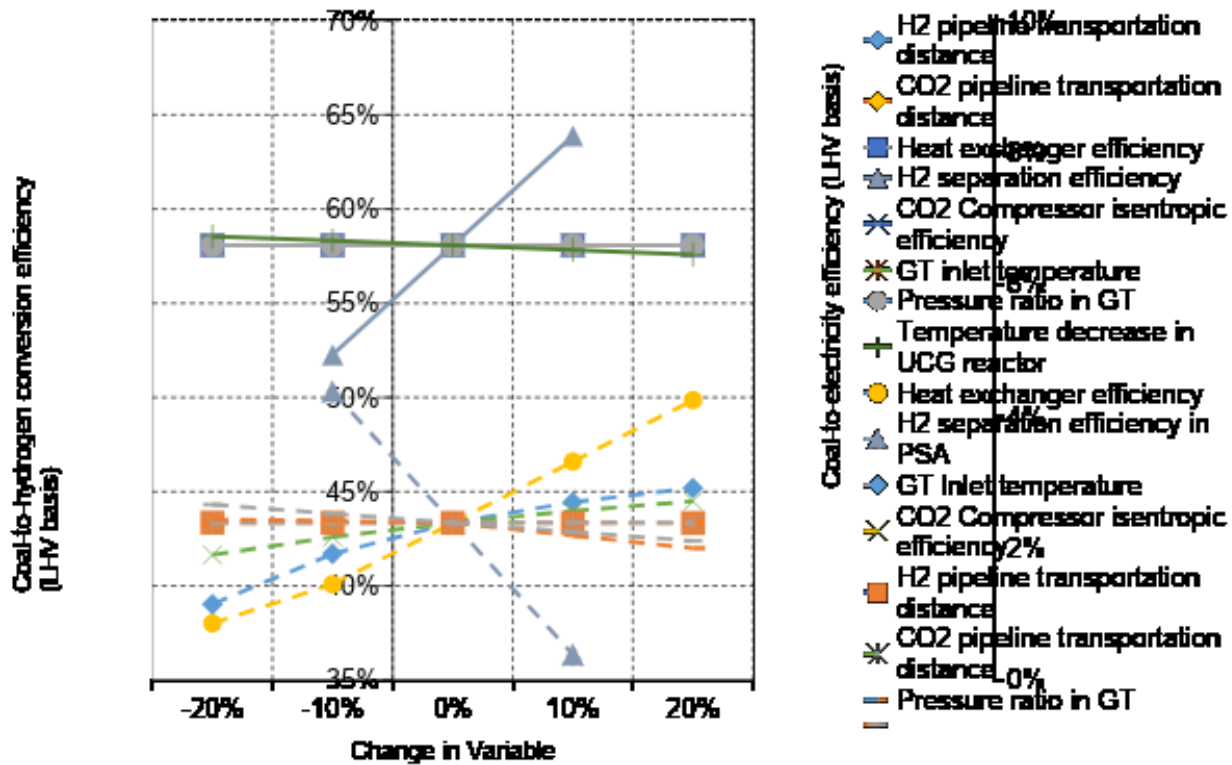


Fig. 7: Sensitivity analysis for H<sub>2</sub> production from UCG with CCS. The H<sub>2</sub>O-to O<sub>2</sub>-ratio is 2, and the ground water influx rate is 0.4 m<sup>3</sup> per tonne coal. Dash lines represent  $\eta_e$ , and solid lines represent  $\eta_h$

## Nomenclature

ASU	air separation unit
bpd	barrels per day
CC	combined cycle
CCS	carbon capture and sequestration
CO <sub>2</sub> e	carbon dioxide equivalent
CRIP	controlled retractable ignition point
ECBM	enhanced coal-bed methane
EOR	enhanced oil recovery
	FUNdamental ENgineering PrinciplEs-based Model for Estimation
FUNNEL-EGY-H2-UCG	of EnerGY consumption and production in hydrogen (H <sub>2</sub> ) production from Underground Coal Gasification
GHG	greenhouse gas
GJ	gigajoule
GT	gas turbine
HP	high pressure
HRSG	heat recovery steam generator
HT	high temperature

HX	heat exchanger
IGCC	integrated gasification combined cycle
kWh	kilowatt hour
LHV	lower heating value
LP	low pressure
LT	low temperature
MDEA	methyl diethanolamine
MEA	monoethanolamine
MPa	megapascal
MW	megawatt
PSA	pressure swing adsorption
SCG	surface coal gasification
SCO	synthetic crude oil
SMR	steam methane reforming
SRR	syngas reforming reactor
SOFC	solid oxide fuel cell
ST	steam turbine
Tt	trillion tons

UCG	underground coal gasification
WGSR	water gas shift reactor
$\eta_e$	electrical energy exported per unit coal energy
$\eta_h$	coal to hydrogen conversion efficiency

**Table 1.**

**Key assumptions in UCG**

Parameter/values		Sources/comments	
Coal Type	High Volatile B Bituminous		[28]
	Manville Coal		
UCG reservoir temperature	60° C		[27]
UCG reservoir pressure	11.5 MPa		[27]
<u>Coal Composition</u>			
Ultimate Analysis		Proximate Analysis	
<i>Parameter</i>	%	<i>Parameter</i>	%
<i>r</i>			
Ash	9.7	Moisture	4.7
Carbon	74.44	Ash	9.3
Hydrogen	3.58	Volatile matter	30.5
Nitrogen	1.1	Fixed carbon	55.5
Sulphur	0.4		
Oxygen	10.7		

LHV of coal (MJ/kg)	28.5	Average of the range 26.8-30.2 MJ/kg [7, 47]
Coal gasified (tonnes/day)	118	[28]
Oxygen injection (tonnes/day)	45	[28]
Water/Oxygen injection mass ratio	2	[28]

**Table 2.**

**Composition of the syngas produced from UCG**

Dry gas mol%					Total	Calorific
					volume of	value of
					dry gas	syngas
CH <sub>4</sub>	CO <sub>2</sub>	CO	H <sub>2</sub>	H <sub>2</sub> S	Nm <sup>3</sup> /hr	MJ/Nm <sup>3</sup>
10.77	20.73	33.69	34.63	0.19	11168.26	10.55
%	%	%	%	%		

**Table 3.****Key assumptions in SRR and WGSR**

<b>Parameter</b>	<b>Value</b>	<b>Sources</b>
<u>SRR</u>		
Steam-to carbon-ratio	3	[43]
Temperature/pressure in SRR, °C/ MPa	800/3	[43]
<u>WGSR</u>		
Pressure loss in WGSRs	4%	[32]
Temperature of gas inlet to HT-WGSR, °C	350	[31]
Temperature of gas outlet from HT-WGSR, °C	450	[31]
Temperature of gas inlet to LT-WGSR, °C	250	[31]
Temperature of gas outlet from LT-WGSR, °C	275	[31]
Pressure loss in HXs	2%	[32]
Temperature of gas inlet for CO <sub>2</sub> absorption, °C	25	[31]

**Table 4.****Key assumptions for CO<sub>2</sub> capture and removal**

Parameter	Value	Sources/comments
<u>CO<sub>2</sub> absorption and removal</u>		
Solvent pump efficiency	75%	[32]
Recycle compressor isentropic efficiency	85%	[40]
Recycle compressor mechanical efficiency	98%	[40]
Pressure in CO <sub>2</sub> absorber, MPa	5	[32]
		Values indicate
Pressure of flash chambers, MPa	1.7, 0.9., 0.32, 0.11	pressure level in chambers 1, 2, 3, and 4, respectively [32]
<u>CO<sub>2</sub> compressor</u>		
Stage 1 discharge pressure, MPa	0.24	[53]
Stage 2 discharge pressure, MPa	0.56	[53]
Stage 3 discharge pressure, MPa	1.3213.2	[53]
Stage 4 discharge pressure, MPa	3.02	[53]
Stage 5 discharge pressure, MPa	7.38	[53]

Booster pump discharge pressure, MPa	15	[53]
Final discharge temperature, °C	25	[53]
Compressor isentropic efficiency	0.75	[53]

**Table 5.**

**Key assumptions for a co-generation plant**

<b>Parameter</b>	<b>Values</b>	<b>Sources/comments</b>
<i><u>Gas turbine</u></i>		
Mechanical efficiency	99.5%	[40]
Polytropic efficiency of turbine	88%	[32]
Polytropic efficiency of compressor	85%	[32]
Ambient air temperature/ pressure, °C/ MPa	15/0.1	[40]
Turbine inlet temperature, °C	1300	[32]
Pressure ratio	14.8	[32]
Turbine outlet pressure	1.1	[40]
Efficiency of electric generator	98.7	[32]

---

Steam turbine

Steam pressure (HP/LP), MPa	3/0.6	Based on steam pressure requirement in SRR, and H <sub>2</sub> S stripper
Isentropic efficiency of turbine	85%	[33]
Mechanical efficiency of turbine	99.5%	[40]
Pump efficiency	75%	[32]
Efficiency of electric generator	98.7%	[32]

---

**Table 6.**

**Key model parameters, output and heat balance for different unit operations in H<sub>2</sub> production from UCG with and without CCS**

Parameter	Values		Comments
	H <sub>2</sub> production	H <sub>2</sub> production	
	with CCS	without CCS	
Coal input (LHV basis), MW <sub>th</sub>	38.92	38.92	
H <sub>2</sub> O-to-O <sub>2</sub> injection ratio	2	2	
Ground water influx, m <sup>3</sup> /tonne of coal	0.4	0.4	
Steam-to-carbon ratio	3	3	Represents the amount of steam required for syngas reforming in SRR, calculated based on the molar flow of carbon (CO+CH <sub>4</sub> ) in the syngas.
<u>Injection</u>			
ASU, MW	0.50	0.50	
Oxygen compression, MW	0.55	0.55	

Water pumping, MW	0.02	0.02	
<u>Expander and H<sub>2</sub>S removal</u>			
Syngas expander, MW	-1.58	-1.58	Negative value indicates power output.
Claus and tail gas treatment plant	0.02	0.02	
<u>CO<sub>2</sub> removal, and transport</u>			
Recycle compressor, MW	0.03	0.03	
Recycle pump, MW	0.39	0.39	
Auxiliary power in CO <sub>2</sub> absorption unit <sup>3</sup> , MW	0.72	0.72	Power consumption of solvent pump and gas compressors.
CO <sub>2</sub> compressor, MW	0.96	0	
CO <sub>2</sub> capture efficiency	91.2%	0	Represents the ratio of the amount of CO <sub>2</sub> captured to the amount of CO <sub>2</sub> in the feed gas.
Purity of captured CO <sub>2</sub> (mol %)	97.4%	0	Remaining gas consists of CH <sub>4</sub> and other gases.
Total CO <sub>2</sub> emissions, kg/hr	1031.3	12207.4	
<u>H<sub>2</sub> separation and transport</u>			

H <sub>2</sub> compressor, MW	0.02	0.02	
<u>Co-generation section</u>			
Gas turbine, MW	-1.16	-1.16	Negative value indicates power output.
Steam turbine, MW	-1.46	-1.46	Negative value indicates power output.
Gross power <sup>6</sup> , MW	-4.20	-4.20	Sum of electricity output from gas turbine, syngas expander, and steam turbine; this value includes auxiliary power consumption (2% of gross power output) and losses in the electrical generator (1.3% of gross power output).
Net power, MW	-0.93	-1.83	Difference of gross power output and electricity requirement in all other unit operations. Also includes a transmission loss of 6.5%. Negative value indicates power output.

H <sub>2</sub> output (LHV basis), MW	22.61	22.61	
H <sub>2</sub> conversion efficiency, $\eta_h$	58.08%	58.08%	See Eq. (1); LHV of H <sub>2</sub> is 120 MJ/kg.
Electrical energy exported per unit coal energy, $\eta_e$	2.39%	4.69%	See Eq. (2).
<hr/> <i>Heat balance</i>			
Heat requirement in SRR, MW	3.28	3.28	This requirement is met by purge gas.
Heat recovered from WGSRs, MW	9.00	9.00	The heat recovered is sent to the co-generation section for steam production. Heat exchanger efficiency is assumed to be 60%.
LP steam to H <sub>2</sub> S stripper, MW	0.04	0.04	This requirement is met by the co-generation section.
HP steam to SRR, MW	9.93	9.93	This requirement is met by the co-generation section.
Heat recovered from CO <sub>2</sub> absorption section, MW	0.99	0.99	The heat recovered is sent to the co-generation section for steam production. Heat exchanger

efficiency is assumed to be 60%.

---

**Table 7.**

**Key performance parameters of H<sub>2</sub> production pathways: UCG, surface coal gasification, and SMR with and without carbon capture**

<b>H<sub>2</sub> production pathway</b>	<b>With or without CCS (CO<sub>2</sub> capture technology)</b>	<b>H<sub>2</sub> conversion efficiency, %</b>	<b>Electrical efficiency<sup>1</sup>, %</b>	<b>CO<sub>2</sub> capture efficiency, %</b>	<b>Sources/ comments</b>
<i>UCG</i>	With CCS (Selexol)	51.4-65.8 <sup>2</sup>	0.8-5.4 <sup>2</sup>	87-95.7 <sup>2</sup>	Present model
	without CCS (Selexol)	51.4-65.8 <sup>2</sup>	3.3-7.6 <sup>2</sup>	0	Present model
<i>SCG</i>	With CCS (Selexol)	51.9	1.4	92	[32, 38]
	Without CCS (Selexol)	51	4.5	0	[32, 38]
	With CCS (Selexol)	44.5	12.8	86.8	[32, 35]

	With CCS (Selexol)	57.3	2.8-3.8 <sup>3</sup>	91.1-91.3 <sup>3</sup>	[32]
	Without CCS (Selexol)	57.5	4.2-6.2 <sup>3</sup>	0	[32]
	With CCS (Selexol)	62	2.3	91	[34]
	With CCS (Selexol)	69	-3.7 <sup>4</sup>	90	[34, 41]
<i>SMR</i>	With CCS (MDEA)	73	0	85	[34, 37]
	With CCS (MEA)	61	-3.9 <sup>4</sup>	90	[34, 42]

<sup>1</sup> Indicates the amount of electrical energy exported per unit coal energy input

<sup>2</sup> Range of values for different ground water influx rates, steam-to-carbon ratio, and H<sub>2</sub>O-to-O<sub>2</sub> injection ratio

<sup>3</sup> The author in [32] present results for different gasification pressures (7-12 MPa) and syngas cooling modes (quench or syngas cooler)

<sup>4</sup> A negative value indicates net import of electricity from the grid



## Appendix A

This appendix consists of screenshots of the Aspen Plus flow sheets, material and energy balances developed for H<sub>2</sub> production from UCG with and without CCS. The model is designed in such a way that the overall H<sub>2</sub> production pathway is sub-divided into various hierarchy blocks. Each hierarchy block represents a unit operation in the H<sub>2</sub> production pathway. The figures in the Appendix represent process flow in a unit operation. On the other hand, the tables in the respective worksheets have the material and energy (heat and work) balances in the unit operation. All the data (temperature, pressure, mass flow, heat flow, work flow, etc.) pertaining to material, heat and work streams in various flow sheets hold true for both scenarios – H<sub>2</sub> production with CCS and H<sub>2</sub> production without CCS.

The table below enlists the features of the eight hierarchy blocks along with the property method used in simulating the unit operation in Aspen Plus. The specifications of the key equipment and material stream flow rates (e.g. coal specification, efficiencies, flow rate of gasifying agents, steam-to-carbon ratio, H<sub>2</sub>O-to-O<sub>2</sub> injection ratio, etc. discussed in the paper) in these hierarchy blocks are input through an MS Excel spreadsheet with the use of Aspen Simulation Workbook. Moreover, the results are extracted from the Aspen flow sheet environment to an MS Excel spreadsheet model to perform the overall energy balances, and H<sub>2</sub> and CO<sub>2</sub> pipeline design.

*Note: Following unit operations are not modelled in Aspen Plus: air separation unit (for injection), sulphur recovery (the CLAUS, SCOT units).*



**Table 1.**

**Hierarchy blocks of the Aspen Plus simulation model**

<b>Block ID**</b>	<b>Block name**</b>	<b>Unit operation*</b>	<b>Property method used</b>	<b>Description</b>
<b>Parent</b>	-	All	-	Parent Aspen Plus simulation flow sheet for H <sub>2</sub> production from UCG. It consists of eight sub-simulation flow sheets called as hierarchy blocks, each of which is exploded in figures in the respective worksheets
<b>Hierarchy Block 1</b>	INJECTIO	Injection	PENG-ROB	Consists of O <sub>2</sub> compression and H <sub>2</sub> O pumping, which are fed into the UCG cavity through the injection well
<b>Hierarchy Block 2</b>	UCG	Underground coal gasification	PENG-ROB	Consists of injection of gasifying agents: H <sub>2</sub> O and O <sub>2</sub> , gasification of coal with the gasifying agents. Ground water influx and temperature decrease due to heat loss to the surrounding strata are considered
<b>Hierarchy Block 3</b>	PIPE-EXP	Syngas expander, syngas cooling and H <sub>2</sub> S removal	PENG-ROB	Consists of syngas expansion and cooling

<b>Hierarchy Block 4</b>	AGR	Syngas expander, syngas cooling and H <sub>2</sub> S removal	PC-SAFT	Consists of H <sub>2</sub> S removal using Selexol before reforming of the syngas
<b>Hierarchy Block 5</b>	SMR-WGSR	Syngas to H <sub>2</sub> conversion	PENG-ROB	Consists of syngas reforming, water gas shift reactions
<b>Hierarchy Block 6</b>	CO <sub>2</sub> -CAP	Selexol CO <sub>2</sub> absorption and removal, H <sub>2</sub> separation	PC-SAFT	Consists of capture of CO <sub>2</sub> using Selexol, compression using 5 stages, PSA unit
<b>Hierarchy Block 7</b>	GT-PGBUR	Co-generation plant	PENG-ROB	Consists of purge gas burner, along with production of electricity by gas turbine
<b>Hierarchy Block 8</b>	HRSG-ST	Co-generation plant	PENG-ROB	Consists of steam generation section along with electricity production by steam turbines

\* Refer to Fig. 1a.

\*\* Refer to Fig. 1b.

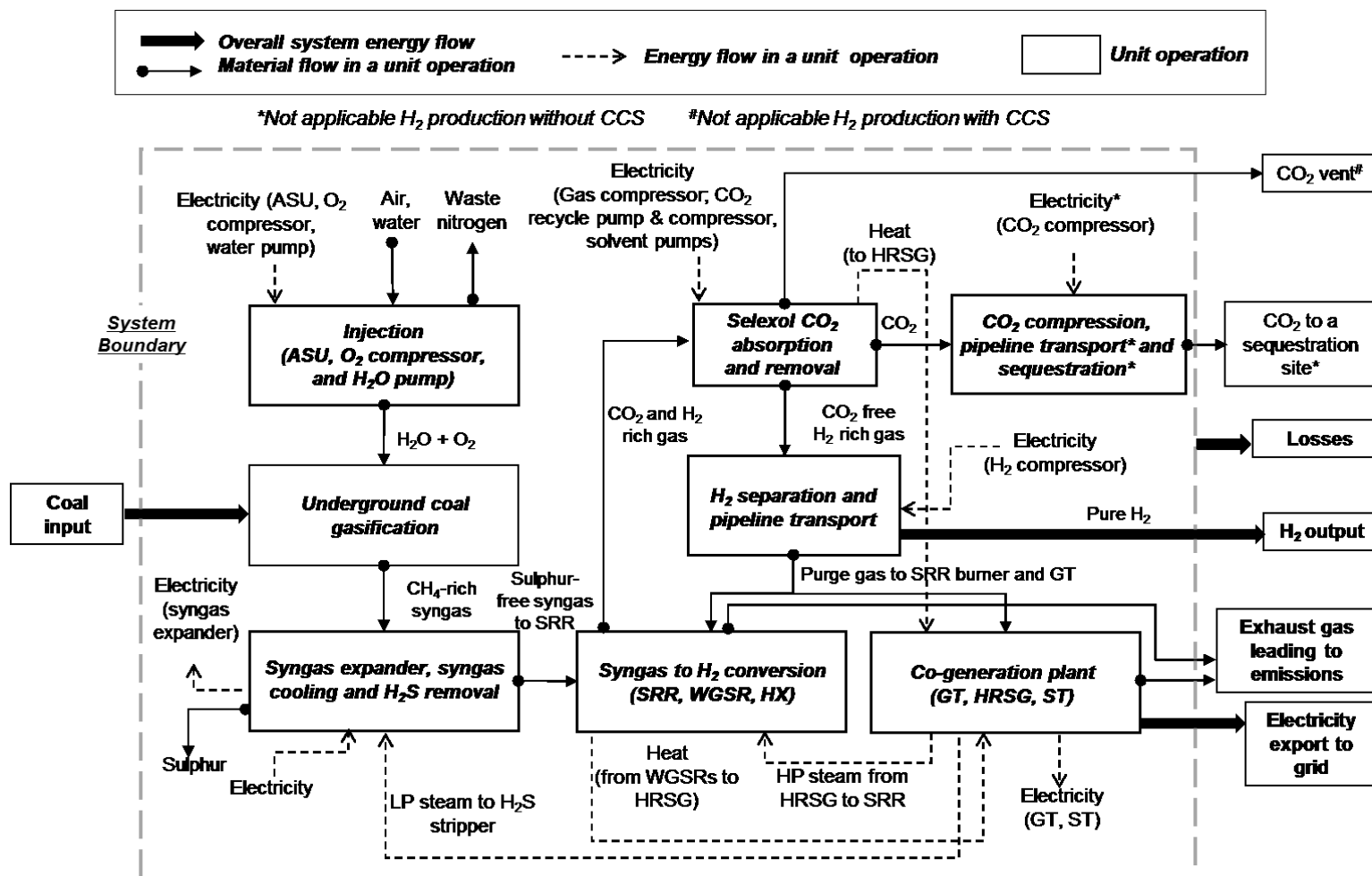
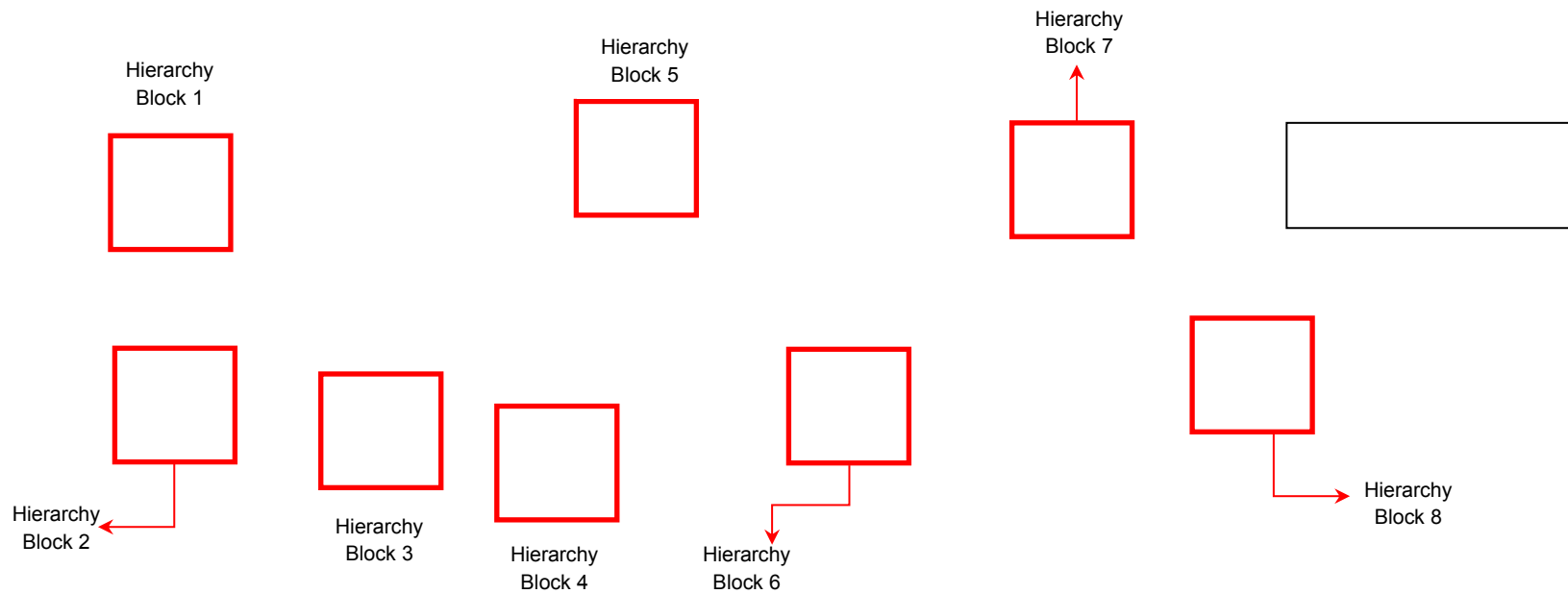


Fig. 1a: Unit operations and system boundary of H<sub>2</sub> production pathways from UCG with CCS and without CCS. All unit operations, except O<sub>2</sub> production in ASU, H<sub>2</sub> separation in PSA and sulphur recovery in Claus unit are modelled in Aspen Plus. Notes: ASU-air separation unit; SRR-syngas reforming reactor; WGSR-water gas shift reactor; HX-heat exchanger; GT-gas turbine; HRSG-heat recovery steam generator; ST-steam turbine.



**Fig. SEQ Figure \\* ARABIC 1b: Parent Aspen Plus simulation flow sheet for H<sub>2</sub> production from UCG. It consists of eight sub-simulation flow sheets called as hierarchy blocks, each of which is exploded in figures below.**

**Table 2a.**

**Material streams in parent simulation flow sheet**

Stream name	ASU-O2	UCG-H2O	H2O	O2	COAL <sup>1</sup>	DRY-GAS	SYNGAS	SYN-H2S	SYN-SMR
Temperature, C	20.0	25.0	26.2	20.0	650.0	25.0	837.2	25.0	9.9
Pressure, bar	1.0	1.0	140.0	200.0	115.0	1.0	106.0	30.0	30.0
Total Mole Flow, kmol/hr	58.6	312.2	312.2	58.6	333.9	429.6	640.2	418.9	400.6
Total Mass Flow, kg/hr	1875.0	5625.0	5625.0	1875.0	4346.4	9926.6	13721.4	9734.4	8985.8
<b>Mass Flow, kg/hr</b>									
CH4	0.0	0.0	0.0	0.0	204.8	1141.7	1141.7	1141.7	1125.5
CO2	0.0	0.0	0.0	0.0	72.6	5959.0	5959.1	5958.1	5273.7
CO	0.0	0.0	0.0	0.0	149.6	2340.3	2340.3	2340.3	2328.8
H2	0.0	0.0	0.0	0.0	21.6	257.1	257.1	257.1	256.8
H2S	0.0	0.0	0.0	0.0	28.3	28.3	28.3	28.2	0.3
H2O	0.0	5625.0	5625.0	0.0	611.4	199.6	3994.4	8.5	0.3
C2H6	0.0	0.0	0.0	0.0	51.8	0.5	0.5	0.5	0.5
N2	0.0	0.0	0.0	0.0	0.0	0.0	0.0	0.0	0.0
DEPG	0.0	0.0	0.0	0.0	0.0	0.0	0.0	0.0	0.0
OXYGEN	1875.0	0.0	0.0	1875.0	0.0	0.0	0.0	0.0	0.0
ARGON	0.0	0.0	0.0	0.0	0.0	0.0	0.0	0.0	0.0
CARBON	0.0	0.0	0.0	0.0	3206.4	0.0	0.0	0.0	0.0

<sup>1</sup> Coal is characterized in the form of its constituents after its pyrolysis

**Table 2b.**

**Material streams in parent simulation flow sheet**

Stream name	CO2-CAP1	CO2-CAP2	LEAN-SEL	CO2-CAP	H2-OUT	PURGGAS	FLUEGAS	HP-STEAM	LP-STEAM	EXHAUST
Temperature, C	25.0	12.8	25.0	25.0	25.0	-2.0	685.5	509.9	302.7	100.0
Pressure, bar	24.0	7.0	1.0	150.0	19.5	1.5	1.1	30.0	6.0	1.1
Total Mole Flow, kmol/hr	644.9	7.0	47.3	231.6	315.3	84.3	616.6	459.9	2.9	616.6
Total Mass Flow, kg/hr	11888.6	272.3	13234.4	9976.7	635.6	637.2	16888.5	8285.8	51.9	16888.5
<b>Mass Flow, kg/hr</b>										
CH4	458.2	13.5	0.0	98.3	0.0	373.2	0.0	0.0	0.0	0.0
CO2	10533.7	246.0	0.0	9869.8	0.0	0.0	1274.5	0.0	0.0	1274.5
CO	146.9	10.8	0.0	5.9	0.0	151.8	0.0	0.0	0.0	0.0
H2	749.4	0.3	0.0	2.0	635.6	112.2	0.0	0.0	0.0	0.0
H2S	0.3	1.3	0.0	0.5	0.0	0.0	0.0	0.0	0.0	0.0
H2O	0.0	0.4	0.0	0.1	0.0	0.0	2038.7	8285.8	51.9	2038.7
C2H6	0.0	0.0	0.0	0.0	0.0	0.0	0.0	0.0	0.0	0.0
N2	0.0	0.0	0.0	0.0	0.0	0.0	11678.4	0.0	0.0	11678.4
DEPG	0.0	0.0	13234.4	0.0	0.0	0.0	0.0	0.0	0.0	0.0
OXYGEN	0.0	0.0	0.0	0.0	0.0	0.0	1623.6	0.0	0.0	1623.6
ARGON	0.0	0.0	0.0	0.0	0.0	0.0	273.3	0.0	0.0	273.3
CARBON	0.0	0.0	0.0	0.0	0.0	0.0	0.0	0.0	0.0	0.0

**Table 3.**

**Heat streams in parent simulation flow sheet**

<b>Stream name</b>	<b>HRSG-2</b>	<b>HRSG-3</b>	<b>HRSG1</b>	<b>SMR-HEAT</b>	<b>TO-SMR</b>	<b>TO-SYN</b>
<b>QCALC, MW</b>	0.95	8.51	7.56	-3.56	3.56	4.17

Negative value indicates heat input; positive value indicates heat output

**Table 4.**

**Work streams in parent simulation flow sheet**

<b>Stream name</b>	<b>ASU</b>	<b>CO2COMP</b>	<b>CO2REM-P</b>	<b>EX-POWER</b>	<b>GROSS-P</b>	<b>GT-POWER</b>	<b>H2OPUMP</b>	<b>PUMP</b>	<b>ST-POWER</b>
<b>POWER, kW</b>	550.45	929.9	1115.70	-1630.10	-4609.29	-1341.62	29.13	5.45	-1637.57

Negative value indicates power output; positive value indicates power input

**Table 5.**

**Block types in the parent Aspen Plus model**

<b>Block name</b>	<b>Type</b>
AGR, CO2-CAP, GT-PGBUR, HRSG-ST, INJECTIO, PIPE-EXP, SMR-WGSR, UCG	Hierarchy
B1, B2	Mixer

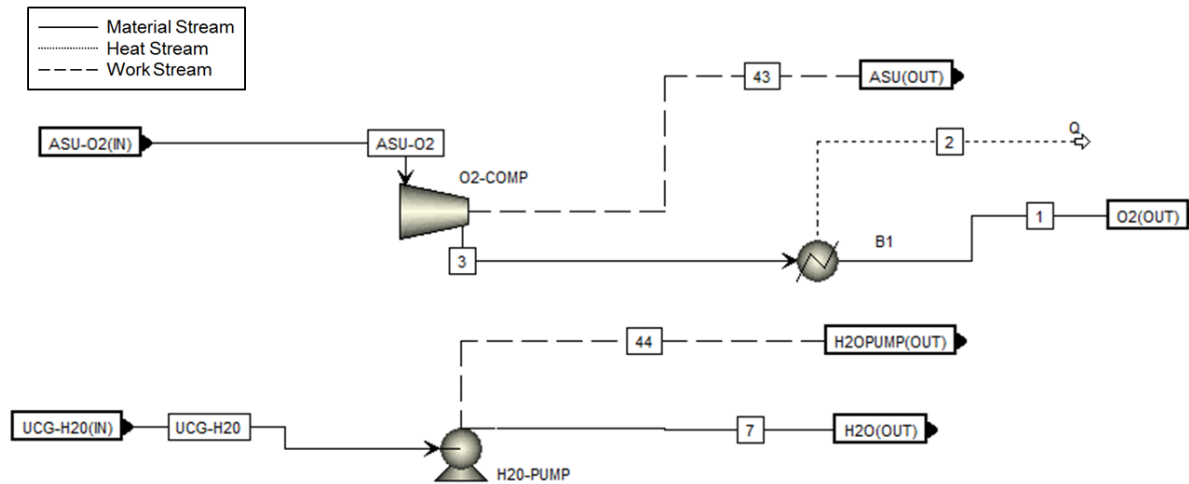


**Fig. 2: Hierarchy Block 1: INJECTIO**

**Table 6.**

**Material streams in Hierarchy Block 1**

Stream name	1	3	7	ASU-O2	UCG-H2O
Temperature, C	20.0	1022.9	26.2	20.0	25.0
Pressure, bar	200.0	200.0	140.0	1.0	1.0

<b>Total Mass Flow, kg/hr</b>	<b>1875.0</b>	<b>1875.0</b>	<b>5625.0</b>	<b>1875.0</b>	<b>5625.0</b>
<b>Mass Flow, kg/hr</b>					
<b>CH4</b>	0.0	0.0	0.0	0.0	0.0
<b>CO2</b>	0.0	0.0	0.0	0.0	0.0
<b>CO</b>	0.0	0.0	0.0	0.0	0.0
<b>H2</b>	0.0	0.0	0.0	0.0	0.0
<b>H2S</b>	0.0	0.0	0.0	0.0	0.0
<b>H2O</b>	0.0	0.0	5625.0	0.0	5625.0
<b>C2H6</b>	0.0	0.0	0.0	0.0	0.0
<b>N2</b>	0.0	0.0	0.0	0.0	0.0
<b>DEPG</b>	0.0	0.0	0.0	0.0	0.0
<b>OXYGEN</b>	1875.0	1875.0	0.0	1875.0	0.0
<b>ARGON</b>	0.0	0.0	0.0	0.0	0.0
<b>CARBON</b>	0.0	0.0	0.0	0.0	0.0

Table 7.

**Work streams in Hierarchy Block 1**

<b>Stream name</b>	<b>43</b>	<b>44</b>
--------------------	-----------	-----------

---

<b>POWER kW</b>	550.4458	29.13168
-----------------	----------	----------

---

Negative value indicates heat input; positive value indicates heat output

**Table 8.**

**Block types in Hierarchy Block 1**

---

<b>Block name</b>	<b>Type</b>
<b>B1</b>	Heater
<b>H2O-PUMP</b>	Pump
<b>O2-COMP</b>	Compr

---

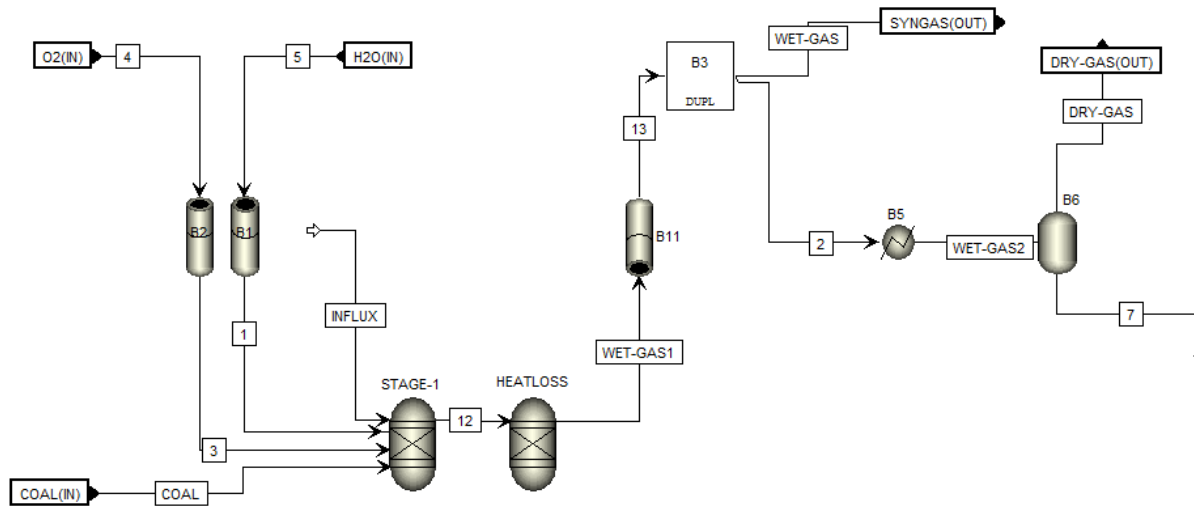


**Fig. 3: Hierarchy Block 2: UCG**

**Table 9.**

**Material streams in Hierarchy Block 2**

Stream name	1	3	7	COAL	INFLUX	WET-GAS1	WET-GAS	DRY-GAS
Temperature, C	26.4	36.0	25.0	650.0	60.0	837.2	837.2	25.0
Pressure, bar	276.3	241.5	1.0	115.0	115.0	115.0	106.0	1.0

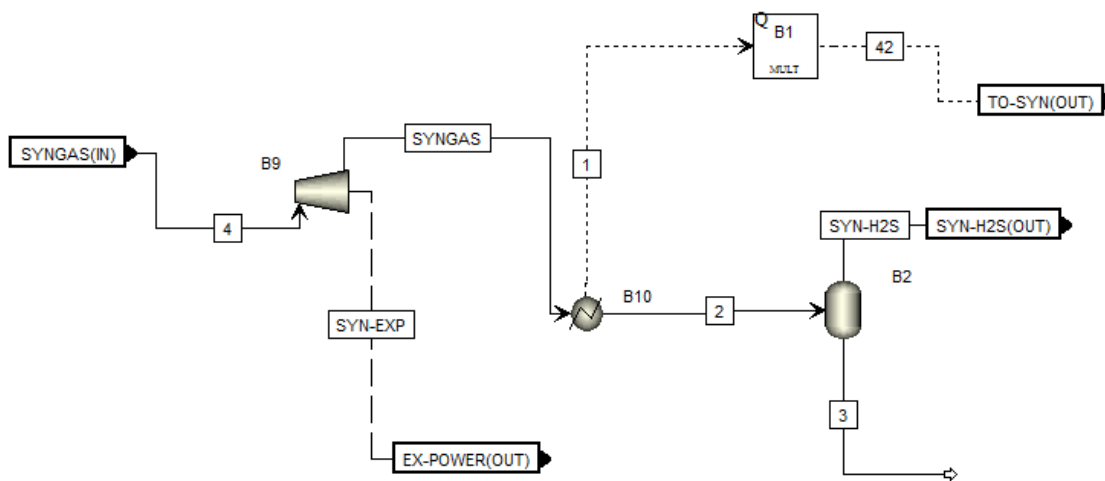
Mass Flow, kg/hr	5625.0	1875.0	3794.8	4346.4	1875.0	13721.4	13721.4	9926.6
<b>Mass Flow, kg/hr</b>								
<b>CH4</b>	0.0	0.0	0.0	204.8	0.0	1141.7	1141.7	1141.7
<b>CO2</b>	0.0	0.0	0.0	72.6	0.0	5959.1	5959.1	5959.0
<b>CO</b>	0.0	0.0	0.0	149.6	0.0	2340.3	2340.3	2340.3
<b>H2</b>	0.0	0.0	0.0	21.6	0.0	257.1	257.1	257.1
<b>H2S</b>	0.0	0.0	0.0	28.3	0.0	28.3	28.3	28.3
<b>H2O</b>	5625.0	0.0	3794.8	611.4	1875.0	3994.4	3994.4	199.6
<b>C2H6</b>	0.0	0.0	0.0	51.8	0.0	0.5	0.5	0.5
<b>N2</b>	0.0	0.0	0.0	0.0	0.0	0.0	0.0	0.0
<b>DEPG</b>	0.0	0.0	0.0	0.0	0.0	0.0	0.0	0.0
<b>OXYGEN</b>	0.0	1875.0	0.0	0.0	0.0	0.0	0.0	0.0
<b>ARGON</b>	0.0	0.0	0.0	0.0	0.0	0.0	0.0	0.0
<b>CARBON</b>	0.0	0.0	0.0	3206.4	0.0	0.0	0.0	0.0

Table 10.

### Block types in Hierarchy Block 2

Block name	Type
<b>B1, B2, B11</b>	Pipe
<b>B3</b>	Dupl
<b>B5</b>	Heater

<b>B6</b>	Flash2
<b>HEATLOSS, STAGE-1</b> RGibbs	



**Fig. 4: Hierarchy Block 3: PIPE-EXP**

Table 11.

Material streams in Hierarchy Block 3

Stream name	SYNGAS	2	3	SYN-H2S
Temperature, C	629.4	25.0	25.0	25.0
Pressure, bar	30.0	30.0	30.0	30.0
Vapor Fraction	1.0	0.7	0.0	1.0
Total Flow, kg/hr	13721.4	13721.4	3987.1	9734.4
<b>Mass Flow, kg/hr</b>				
CH4	1141.7	1141.7	0.0	1141.7
CO2	5959.1	5959.1	1.0	5958.1
CO	2340.3	2340.3	0.0	2340.3
H2	257.1	257.1	0.0	257.1
H2S	28.3	28.3	0.2	28.2
H2O	3994.4	3994.4	3985.9	8.5
C2H6	0.5	0.5	0.0	0.5
N2	0.0	0.0	0.0	0.0
DEPG	0.0	0.0	0.0	0.0
OXYGEN	0.0	0.0	0.0	0.0
ARGON	0.0	0.0	0.0	0.0
CARBON	0.0	0.0	0.0	0.0

**Table 12.**

**Heat streams in Hierarchy Block 3**

<b>Stream name</b>	<b>1</b>	<b>42</b>
<b>QCALC, MW</b>	6.9	4.2

Negative value indicates heat input; positive value indicates heat output

**Table 13.**

**Work streams in Hierarchy Block 3**

<b>Stream name</b>	<b>SYN-EXP</b>
<b>POWER kW</b>	-1630.1

Negative value indicates power output; positive value indicates power input

**Table 14.**

**Block types in Hierarchy Block 3**

<b>Block name</b>	<b>Type</b>
<b>B1</b>	Mult
<b>B2</b>	Flash2
<b>B9</b>	Compr
<b>B10</b>	Heater

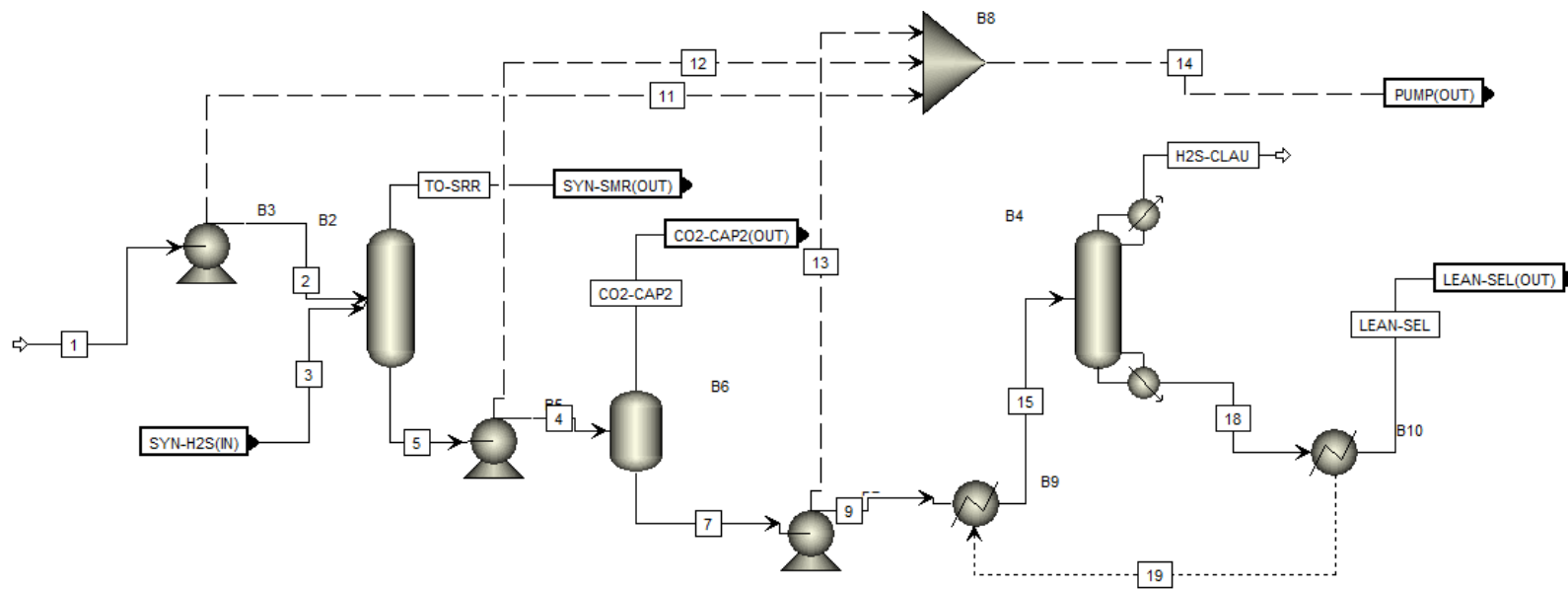


**Fig. 5: Hierarchy Block 4: AGR**

**Table 15.**

**Material streams in Hierarchy Block 4**

Stream name	1	2	4	5	7	9	15	18	CO2-CAP2	H2S-CLAU	LEAN-SEL	TO-SRR
Temperature, C	0.0	0.7	15.6	15.7	12.8	12.8	273.8	316.4	12.8	269.9	25.0	9.9
Pressure, bar	1.0	30.0	7.0	30.0	7.0	1.0	1.0	1.0	7.0	1.0	1.0	30.0

<b>Vapor Fraction</b>	0.0	0.0	0.0	0.0	0.0	0.0	0.3	0.0	1.0	1.0	0.0	1.0
<b>Total Flow, kg/hr</b>	14461.9	14461.9	15210.5	15210.5	14938.2	14938.2	14938.2	13234.4	272.3	1703.8	13234.4	8985.8
<b>Mass Flow, kg/hr</b>												
<b>CH4</b>	0.0	0.0	16.2	16.2	2.7	2.7	2.7	0.0	13.5	2.7	0.0	1125.5
<b>CO2</b>	0.0	0.0	684.4	684.4	438.4	438.4	438.4	0.0	246.0	438.4	0.0	5273.7
<b>CO</b>	0.0	0.0	11.5	11.5	0.7	0.7	0.7	0.0	10.8	0.7	0.0	2328.8
<b>H2</b>	0.0	0.0	0.3	0.3	0.0	0.0	0.0	0.0	0.3	0.0	0.0	256.8
<b>H2S</b>	0.0	0.0	27.9	27.9	26.6	26.6	26.6	0.0	1.3	26.6	0.0	0.3
<b>H2O</b>	0.0	0.0	8.2	8.2	7.8	7.8	7.8	0.0	0.4	7.8	0.0	0.3
<b>C2H6</b>	0.0	0.0	0.1	0.1	0.0	0.0	0.0	0.0	0.0	0.0	0.0	0.5
<b>N2</b>	0.0	0.0	0.0	0.0	0.0	0.0	0.0	0.0	0.0	0.0	0.0	0.0
<b>DEPG</b>	14461.9	14461.9	14461.9	14461.9	14461.9	14461.9	14461.9	13234.4	0.0	1227.5	13234.4	0.0
<b>OXYGEN</b>	0.0	0.0	0.0	0.0	0.0	0.0	0.0	0.0	0.0	0.0	0.0	0.0
<b>ARGON</b>	0.0	0.0	0.0	0.0	0.0	0.0	0.0	0.0	0.0	0.0	0.0	0.0
<b>CARBON</b>	0.0	0.0	0.0	0.0	0.0	0.0	0.0	0.0	0.0	0.0	0.0	0.0

**Table 16.**

**Work streams in Hierarchy Block 4**

<b>Stream name</b>	<b>11</b>	<b>12</b>	<b>13</b>	<b>14</b>
<b>POWER, kW</b>	13.7	-6.6	-1.7	5.4

Negative value indicates power output; positive value indicates power input

**Table 17.**

**Block types in Hierarchy Block 4**

<b>Block name</b>	<b>Type</b>
<b>B6</b>	Flash2
<b>B9, B10</b>	Heater
<b>B8</b>	Mixer
<b>B3, B5, B7</b>	Pump
<b>B2, B4</b>	RadFrac

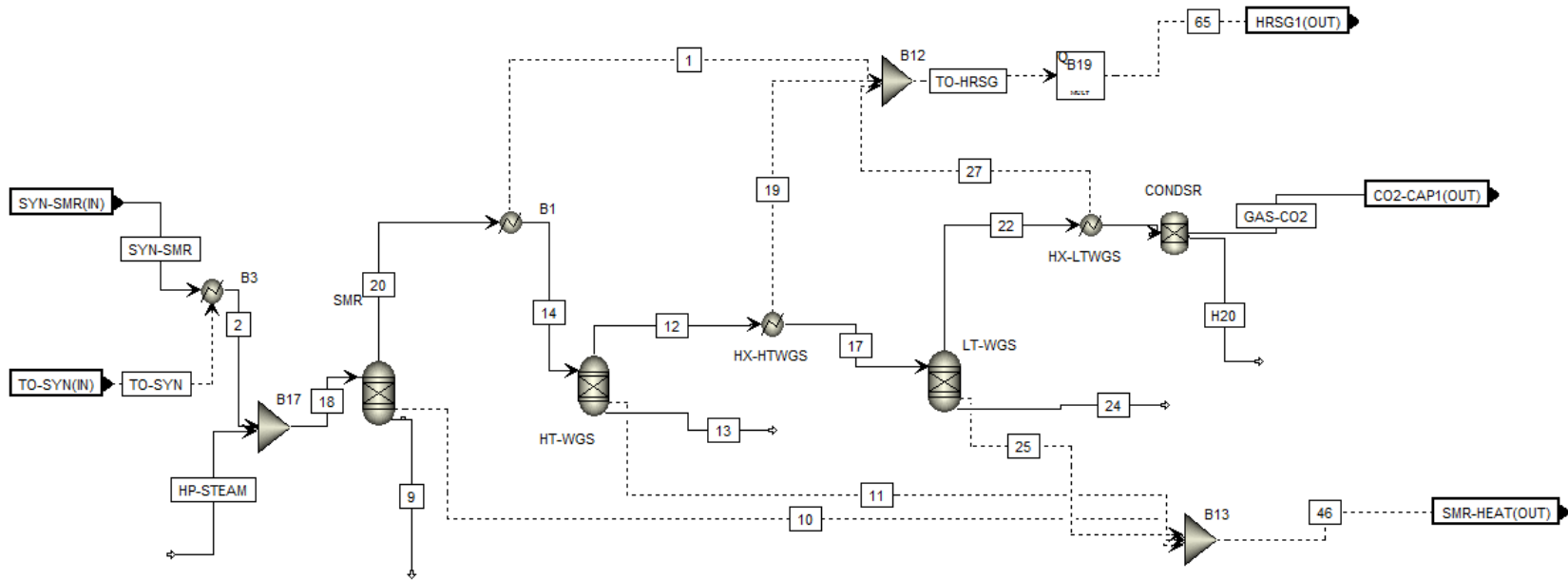


**Fig. 6: Hierarchy Block 5: SMR-WGSR**

**Table 18.**

**Material streams in Hierarchy Block 5**

Stream name	2	20	14	12	17	22	26	GAS-CO2	H2O	HP-STEAM
-------------	---	----	----	----	----	----	----	---------	-----	----------

<b>Temperature, C</b>	916.0	800.0	350.0	450.0	250.0	275.0	25.0	25.0	25.0	510.0
<b>Pressure, bar</b>	29.4	27.7	27.1	26.0	25.5	24.5	24.0	24.0	24.0	30.0
<b>Vapor Fraction</b>	1.0	1.0	1.0	1.0	1.0	1.0	0.7	1.0	0.0	1.0
<b>Total Flow, kg/hr</b>	8985.8	17271.6	17271.6	17271.6	17271.6	17271.6	17271.6	11888.6	5383.1	8285.8
<b>Mass Flow, kg/hr</b>										
<b>CH4</b>	1125.5	458.2	458.2	458.2	458.2	458.2	458.2	458.2	0.0	0.0
<b>CO2</b>	5273.7	6473.9	6473.9	9422.9	9422.9	10533.7	10533.7	10533.7	0.0	0.0
<b>CO</b>	2328.8	2730.8	2730.8	853.9	853.9	146.9	146.9	146.9	0.0	0.0
<b>H2</b>	256.8	563.5	563.5	698.5	698.5	749.4	749.4	749.4	0.0	0.0
<b>H2S</b>	0.3	0.3	0.3	0.3	0.3	0.3	0.3	0.3	0.0	0.0
<b>H2O</b>	0.3	7045.0	7045.0	5837.8	5837.8	5383.1	5383.1	0.0	5383.1	8285.8
<b>C2H6</b>	0.5	0.0	0.0	0.0	0.0	0.0	0.0	0.0	0.0	0.0
<b>N2</b>	0.0	0.0	0.0	0.0	0.0	0.0	0.0	0.0	0.0	0.0
<b>DEPG</b>	0.0	0.0	0.0	0.0	0.0	0.0	0.0	0.0	0.0	0.0
<b>OXYGEN</b>	0.0	0.0	0.0	0.0	0.0	0.0	0.0	0.0	0.0	0.0
<b>ARGON</b>	0.0	0.0	0.0	0.0	0.0	0.0	0.0	0.0	0.0	0.0
<b>CARBON</b>	0.0	0.0	0.0	0.0	0.0	0.0	0.0	0.0	0.0	0.0

**Table 19.**

**Heat streams in Hierarchy Block 5**

<b>Stream name</b>	<b>1</b>	<b>10</b>	<b>11</b>	<b>19</b>	<b>25</b>	<b>27</b>	<b>46</b>	<b>65</b>	<b>TO-HRSG</b>	<b>TO-SYN</b>
<b>QCALC , MW</b>	4.6	-3.3	-0.3	2.0	0.0	6.0	-3.6	7.6	12.6	4.2

Negative value indicates heat input; positive value indicates heat output

**Table 20.**

**Block types in Hierarchy Block 5**

<b>Block name</b>	<b>Type</b>
<b>B1, B3, HX-HTWGS, HX-LTWGS</b>	Heater
<b>B12, B13, B17</b>	Mixer
<b>B19</b>	Mult
<b>HT-WGS, LT-WGS, SMR</b>	
<b>CONDSR</b>	Sep

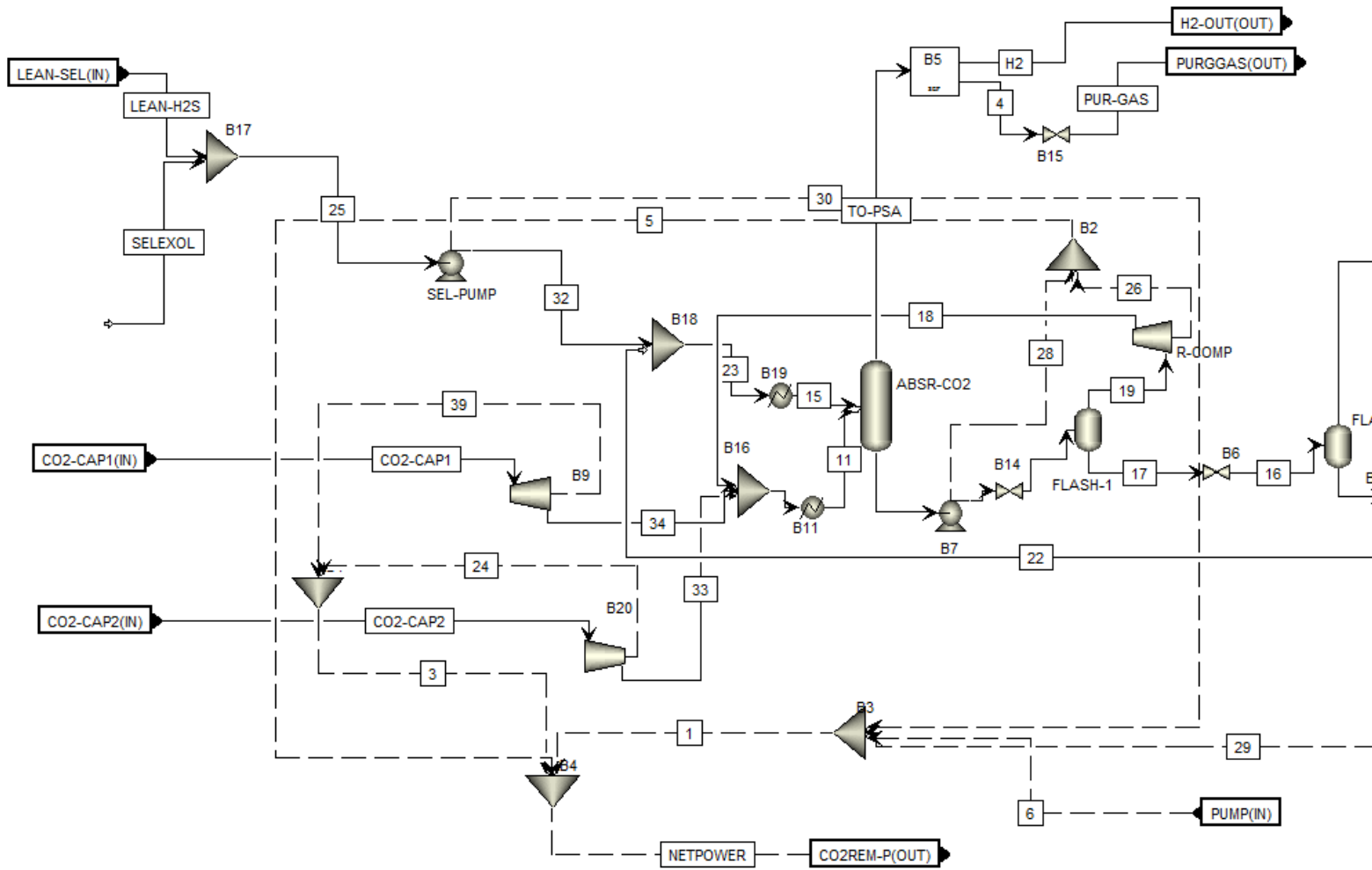
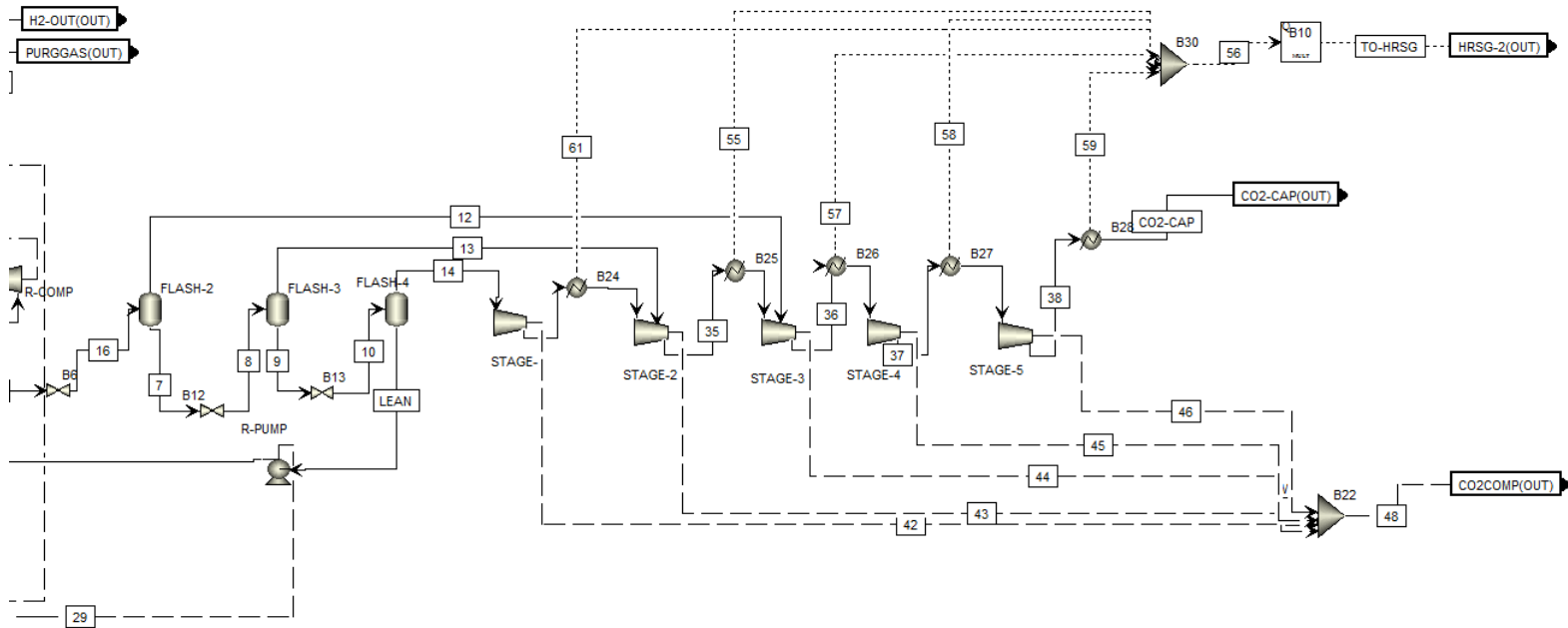


Fig. 7a: Hierarchy Block 6: CO2-CAP (consists of CO<sub>2</sub> capture using Selexol, portion of Selexol flash)



**Fig. 7b: Hierarchy Block 6: CO<sub>2</sub>-CAP (consists of Selexol flash and CO<sub>2</sub> compression)**

Table 21a.

**Material streams in Hierarchy Block 6**

Stream name	2	7	8	9	10	11	12	13	14	15	16	17
Temperature, C	9.9	25.0	21.5	25.0	23.7	25.0	25.0	25.0	25.0	0.0	23.6	25.0
Pressure, bar	17.0	9.5	3.2	3.2	1.1	50.0	9.5	3.2	1.1	50.0	9.5	17.0
Vapor Fraction	0.0	0.0	0.1	0.0	0.0	1.0	1.0	1.0	1.0	0.0	0.1	0.0
Total Flow, kg/hr	242625. 7	238755. 5	238755. 5	233311. 1	233311. 1	13355. 3	2676. 7	5444. 4	1855. 6	230543. 2	241432. 2	241432. 2
Mass Flow, kg/hr												
CH4	164.9	31.5	31.5	2.2	2.2	538.2	67.0	29.3	2.0	0.0	98.5	98.5
CO2	11881.2	8178.0	8178.0	2764.0	2764.0	11881. 2	2602. 6	5413. 9	1853. 3	0.0	10780.5	10780.5
CO	17.2	0.8	0.8	0.0	0.0	169.0	5.1	0.8	0.0	0.0	5.9	5.9
H2	17.2	0.1	0.1	0.0	0.0	764.9	1.9	0.1	0.0	0.0	2.0	2.0
H2S	1.6	1.5	1.5	1.3	1.3	1.6	0.0	0.2	0.2	0.0	1.5	1.5
H2O	0.4	0.4	0.4	0.4	0.4	0.4	0.0	0.1	0.1	0.0	0.4	0.4
C2H6	0.1	0.0	0.0	0.0	0.0	0.1	0.0	0.0	0.0	0.0	0.1	0.1
N2	0.0	0.0	0.0	0.0	0.0	0.0	0.0	0.0	0.0	0.0	0.0	0.0
DEPG	230543. 2	230543. 2	230543. 2	230543. 2	230543. 2	0.0	0.0	0.0	0.0	230543. 2	230543. 2	230543. 2

<b>OXYGEN</b>	0.0	0.0	0.0	0.0	0.0	0.0	0.0	0.0	0.0	0.0	0.0	0.0
<b>ARGON</b>	0.0	0.0	0.0	0.0	0.0	0.0	0.0	0.0	0.0	0.0	0.0	0.0
<b>CARBON</b>	0.0	0.0	0.0	0.0	0.0	0.0	0.0	0.0	0.0	0.0	0.0	0.0

**Table 21b.**

**Material streams in Hierarchy Block 6**

<b>Stream name</b>	<b>19</b>	<b>20</b>	<b>21</b>	<b>27</b>	<b>31</b>	<b>32</b>	<b>18</b>	<b>33</b>	<b>34</b>	<b>35</b>	<b>36</b>	<b>37</b>
<b>Temperature, C</b>	25.0	97.4	10.0	9.9	101.8	26.2	124.4	192.8	94.6	105.1	109.4	110.4
<b>Pressure, bar</b>	17.0	50.0	50.0	23.0	2.4	50.0	50.0	50.0	50.0	5.6	13.2	30.2
<b>Vapor Fraction</b>	1.0	1.0	0.0	0.0	1.0	0.0	1.0	1.0	1.0	1.0	1.0	1.0
<b>Total Flow, kg/hr</b>	1193.5	13354.4	242625.7	242625.7	1855.6	230543.2	1193.5	272.3	11888.6	7300.0	9976.7	9976.7
<b>Mass Flow, kg/hr</b>												
<b>CH4</b>	66.5	538.2	164.9	164.9	2.0	0.0	66.5	13.5	458.2	31.3	98.3	98.3
<b>CO2</b>	1100.6	11880.3	11881.2	11881.2	1853.3	0.0	1100.6	246.0	10533.7	7267.2	9869.8	9869.8
<b>CO</b>	11.2	169.0	17.2	17.2	0.0	0.0	11.2	10.8	146.9	0.8	5.9	5.9
<b>H2</b>	15.2	764.9	17.2	17.2	0.0	0.0	15.2	0.3	749.4	0.1	2.0	2.0
<b>H2S</b>	0.0	1.6	1.6	1.6	0.2	0.0	0.0	1.3	0.3	0.4	0.5	0.5

<b>H2O</b>	0.0	0.4	0.4	0.4	0.1	0.0	0.0	0.4	0.0	0.1	0.1	0.1
<b>C2H6</b>	0.0	0.1	0.1	0.1	0.0	0.0	0.0	0.0	0.0	0.0	0.0	0.0
<b>N2</b>	0.0	0.0	0.0	0.0	0.0	0.0	0.0	0.0	0.0	0.0	0.0	0.0
<b>DEPG</b>	0.0	0.0	230543.2	230543.2	0.0	230543.2	0.0	0.0	0.0	0.0	0.0	0.0
<b>OXYGEN</b>	0.0	0.0	0.0	0.0	0.0	0.0	0.0	0.0	0.0	0.0	0.0	0.0
<b>ARGON</b>	0.0	0.0	0.0	0.0	0.0	0.0	0.0	0.0	0.0	0.0	0.0	0.0
<b>CARBON</b>	0.0	0.0	0.0	0.0	0.0	0.0	0.0	0.0	0.0	0.0	0.0	0.0

**Table 21c.**

**Material streams in Hierarchy Block 6**

Stream name	38	49	50	51	52	CO2-CAP	H2	22	LEAN	23	PUR-GAS	SELEXOL	TO-PSA
<b>Temperature, C</b>	196.7	31.1	31.1	31.1	31.1	25.0	25	26.2	25.0	26.2	-2.0	25.0	-0.1
<b>Pressure, bar</b>	150.0	2.4	5.6	13.2	30.2	150.0	19.5	50.0	1.1	50.0	1.5	1.0	50.0
<b>Vapor Fraction</b>	1.0	1.0	1.0	1.0	1.0	0.0	1.0	0.0	0.0	0.0	1.0	0.0	1.0
<b>Total Flow, kg/hr</b>	9976.7	1855.6	7300.0	9976.7	9976.7	9976.7	635.6	231455.5	231455.5	230543.2	637.2	217308.8	1272.8
<b>Mass Flow, kg/hr</b>													
<b>CH4</b>	98.3	2.0	31.3	98.3	98.3	98.3	0.0	0.1	0.1	0.0	373.2	0.0	373.2
<b>CO2</b>	9869.8	1853.3	7267.2	9869.8	9869.8	9869.8	0.0	910.7	910.7	0.0	0.0	0.0	0.0
<b>CO</b>	5.9	0.0	0.8	5.9	5.9	5.9	0.0	0.0	0.0	0.0	151.8	0.0	151.8

<b>H2</b>	2.0	0.0	0.1	2.0	2.0	2.0	635.6	0.0	0.0	0.0	112.2	0.0	747.8
<b>H2S</b>	0.5	0.2	0.4	0.5	0.5	0.5	0.0	1.1	1.1	0.0	0.0	0.0	0.0
<b>H2O</b>	0.1	0.1	0.1	0.1	0.1	0.1	0.0	0.3	0.3	0.0	0.0	0.0	0.0
<b>C2H6</b>	0.0	0.0	0.0	0.0	0.0	0.0	0.0	0.0	0.0	0.0	0.0	0.0	0.0
<b>N2</b>	0.0	0.0	0.0	0.0	0.0	0.0	0.0	0.0	0.0	0.0	0.0	0.0	0.0
<b>DEPG</b>	0.0	0.0	0.0	0.0	0.0	0.0	0.0	230543.3	230543.3	230543.2	0.0	217308.8	0.0
<b>OXYGEN</b>	0.0	0.0	0.0	0.0	0.0	0.0	0.0	0.0	0.0	0.0	0.0	0.0	0.0
<b>ARGON</b>	0.0	0.0	0.0	0.0	0.0	0.0	0.0	0.0	0.0	0.0	0.0	0.0	0.0
<b>CARBON</b>	0.0	0.0	0.0	0.0	0.0	0.0	0.0	0.0	0.0	0.0	0.0	0.0	0.0

**Table 22.**

**Heat streams in Hierarchy Block 6**

<b>Stream name</b>	<b>55</b>	<b>56</b>	<b>57</b>	<b>58</b>	<b>59</b>	<b>61</b>	<b>TO-HRSG</b>
<b>QCALC, MW</b>	0.1	1.6	0.2	0.2	1.0	0.0	1.0

Negative value indicates heat input; positive value indicates heat output

**Table 23.**

**Work streams in Hierarchy Block 6**

Stream name	1	3	5	6	24	26	28	29	30	39	42	43	44	45	46	48	NETPOWER
<b>POWER, kW</b>	761.8	439.6	-85.7	5.4	13.2	36.0	-121.7	378.8	377.5	426.4	35.6	144.3	200.9	187.5	361.6	929.9	1115.7

Negative value indicates power output; positive value indicates power input

**Table 24.**

**Block types in Hierarchy Block 6**

Block name	Type
<b>B9, B20, R-COMP, STAGE-1, STAGE-2, STAGE-3, STAGE-4, STAGE-5</b>	Compr
<b>FLASH-1, FLASH-2, FLASH-3, FLASH-4</b>	Flash 2
<b>B11, B19, B24, B25, B26, B27, B28</b>	Heater
<b>B16, B17, B18, B1, B2, B3, B4, B22, B30</b>	Mixer
<b>B10</b>	Mult
<b>R-PUMP, SEL-PUMP, B7</b>	Pump



**Table 25.**

**Material streams in Hierarchy Block 7**

<b>Stream name</b>	<b>2</b>	<b>3</b>	<b>4</b>	<b>5</b>	<b>6</b>	<b>7</b>	<b>14</b>	<b>AIR</b>	<b>FLUEGAS1</b>	<b>WATER</b>
<b>Temperature, C</b>	15.0	-2.0	115.1	351.6	397.7	1299.9	256.2	15.0	685.5	164.3
<b>Pressure, bar</b>	1.0	1.5	14.8	14.8	15.0	14.8	14.8	1.0	1.1	14.8
<b>Vapor Fraction</b>	1.0	1.0	1.0	1.0	1.0	1.0	1.0	1.0	1.0	0.0
<b>Total Flow, kg/hr</b>	16053.2	637.2	835.4	16888.5	16053.2	16888.5	637.2	9679.5	16888.5	198.2
<b>Mass Flow, kg/hr</b>										
<b>CH4</b>	0.0	373.2	373.2	373.2	0.0	0.0	373.2	0.0	0.0	0.0
<b>CO2</b>	12.1	0.0	0.0	12.2	12.1	1274.5	0.0	7.3	1274.5	0.0
<b>CO</b>	0.0	151.8	151.8	151.8	0.0	0.0	151.8	0.0	0.0	0.0
<b>H2</b>	0.0	112.2	112.2	112.2	0.0	0.0	112.2	0.0	0.0	0.0
<b>H2S</b>	0.0	0.0	0.0	0.0	0.0	0.0	0.0	0.0	0.0	0.0
<b>H2O</b>	0.0	0.0	198.2	198.2	0.0	2038.7	0.0	0.0	2038.7	198.2
<b>C2H6</b>	0.0	0.0	0.0	0.0	0.0	0.0	0.0	0.0	0.0	0.0
<b>N2</b>	11678.4	0.0	0.0	11678.4	11678.4	11678.4	0.0	7041.6	11678.4	0.0
<b>DEPG</b>	0.0	0.0	0.0	0.0	0.0	0.0	0.0	0.0	0.0	0.0
<b>OXYGEN</b>	4089.3	0.0	0.0	4089.3	4089.3	1623.6	0.0	2465.7	1623.6	0.0
<b>ARGON</b>	273.3	0.0	0.0	273.3	273.3	273.3	0.0	164.8	273.3	0.0
<b>CARBON</b>	0.0	0.0	0.0	0.0	0.0	0.0	0.0	0.0	0.0	0.0

**Table 26.**

**Heat streams in Hierarchy Block 7**

<b>Stream name</b>	<b>1</b>
<b>QCALC, MW</b>	3.6

Negative value indicates heat input; positive value indicates heat output

**Table 27.**

**Work streams in Hierarchy Block 7**

<b>Stream name</b>	<b>10</b>	<b>11</b>	<b>15</b>	<b>GT-POWER</b>
<b>POWER, kW</b>	2333.5	-3872.2	197.1	-1341.6

Negative value indicates power output; positive value indicates power input

**Table 28.**

**Block types in Hierarchy Block 7**

<b>Block name</b>	<b>Type</b>
<b>B1, B2, B6</b>	Mixer
<b>B4</b>	Mult
<b>COMBUSTE</b>	RStoich
<b>B3, GAS-TURB, PG-COMP</b>	Compr

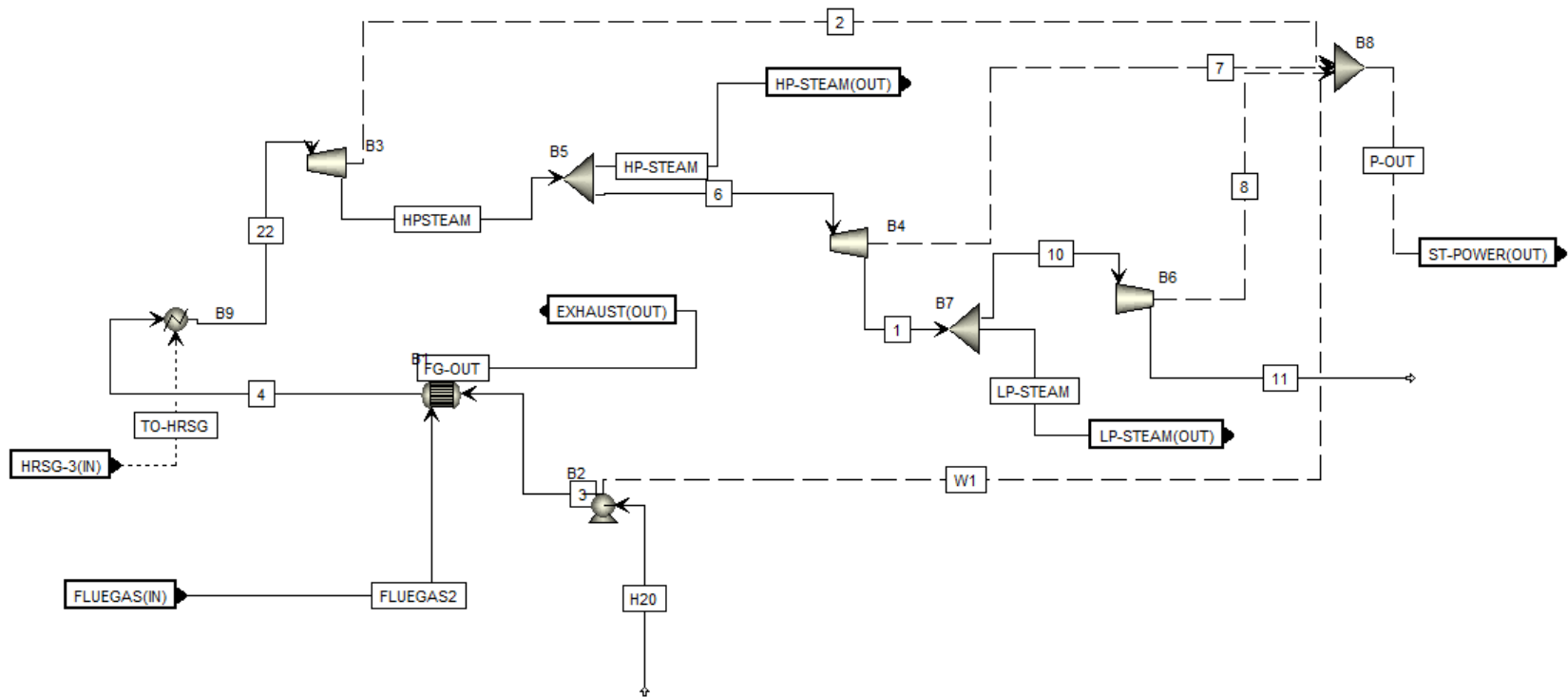


**Fig. 9: Hierarchy Block 8: HRSG-ST**

**Table 29.**

**Material streams in Hierarchy Block 8**

<b>Stream name</b>	<b>1</b>	<b>3</b>	<b>4</b>	<b>6</b>	<b>10</b>	<b>11</b>	<b>22</b>	<b>FG-OUT</b>	<b>FLUEGAS2</b>	<b>H2O</b>	<b>HP-STEAM</b>	<b>LP-STEAM</b>
<b>Temperature, C</b>	302.7	25.9	248.7	509.9	302.7	164.3	702.0	100.0	685.5	25.0	509.9	302.7
<b>Pressure, bar</b>	6.0	100.0	100.0	30.0	6.0	1.5	97.5	1.1	1.1	1.0	30.0	6.0
<b>Vapor Fraction</b>	1.0	0.0	0.0	1.0	1.0	1.0	1.0	1.0	1.0	0.0	1.0	1.0
<b>Total Flow, kg/hr</b>	2752.4	11038.3	11038.3	2752.4	2700.5	2700.5	11038.3	16888.5	16888.5	11038.3	8285.8	51.9
<b>Mass Flow, kg/hr</b>												
<b>CH4</b>	0.0	0.0	0.0	0.0	0.0	0.0	0.0	0.0	0.0	0.0	0.0	0.0
<b>CO2</b>	0.0	0.0	0.0	0.0	0.0	0.0	0.0	1274.5	1274.5	0.0	0.0	0.0
<b>CO</b>	0.0	0.0	0.0	0.0	0.0	0.0	0.0	0.0	0.0	0.0	0.0	0.0
<b>H2</b>	0.0	0.0	0.0	0.0	0.0	0.0	0.0	0.0	0.0	0.0	0.0	0.0
<b>H2S</b>	0.0	0.0	0.0	0.0	0.0	0.0	0.0	0.0	0.0	0.0	0.0	0.0
<b>H2O</b>	2752.4	11038.3	11038.3	2752.4	2700.5	2700.5	11038.3	2038.7	2038.7	11038.3	8285.8	51.9
<b>C2H6</b>	0.0	0.0	0.0	0.0	0.0	0.0	0.0	0.0	0.0	0.0	0.0	0.0
<b>N2</b>	0.0	0.0	0.0	0.0	0.0	0.0	0.0	11678.4	11678.4	0.0	0.0	0.0
<b>DEPG</b>	0.0	0.0	0.0	0.0	0.0	0.0	0.0	0.0	0.0	0.0	0.0	0.0
<b>OXYGEN</b>	0.0	0.0	0.0	0.0	0.0	0.0	0.0	1623.6	1623.6	0.0	0.0	0.0
<b>ARGON</b>	0.0	0.0	0.0	0.0	0.0	0.0	0.0	273.3	273.3	0.0	0.0	0.0
<b>CARBON</b>	0.0	0.0	0.0	0.0	0.0	0.0	0.0	0.0	0.0	0.0	0.0	0.0

**Table 30.**

**Work streams in Hierarchy Block 8**

<b>Stream name</b>	<b>2</b>	<b>7</b>	<b>8</b>	<b>P-OUT</b>	<b>W1</b>
<b>POWER, kW</b>	-1173.9	-307.7	-196.7	-1637.6	40.7

Negative value indicates power output; positive value indicates power input

**Table 31.**

**Block types in Hierarchy Block 8**

<b>Block name</b>	<b>Type</b>
<b>B1</b>	HeatX
<b>B2</b>	Pump
<b>B3, B4, B6</b>	Compr
<b>B5, B7</b>	FSplit

<b>B8</b>	Mixer
<b>B9</b>	Heater